6-26-2015

Calcium Signaling Dynamics in RBL Cells Under Pulsed Ligand Exposure

Mario Paz

Mario J. Paz

Candidate

Nanoscience and Microsystems

Department

This thesis is approved, and it is acceptable in quality and form for publication:

Approved by the Thesis Committee:

Dr. Diane Lidke , Chairperson

Dr. Conrad James

Dr. Deborah Evans

Dr. Eva Chi

Calcium Signaling Dynamics in RBL Cells Under Pulsed Ligand Exposure

by

MARIO J. PAZ

B.S. MECHANICAL ENGINEERING, UNIVERSITY OF NEW MEXICO, 2006

THESIS

Submitted in Partial Fulfillment of the
Requirements for the Degree of

Master of Science
Nanoscience and Microsystems Engineering

The University of New Mexico
Albuquerque, New Mexico
December 2014

Acknowledgements:

I would like to first and for most thank my committee chair, mentor, advisor, and friend Dr. Diane Lidke. Without her all of this would not be possible. She provided an environment to gain a wealth of knowledge and discovery. I also would like to thank my committee members Dr. Eva Chi, and Dr. Debi Evans, you had a close hand in the thesis guidance process.

I would like to thank my co-advisor, and mentor Dr. Conrad James, his knowledge of microfluidics and science is invaluable and appreciated greatly. I would also like to thank our collaborators at Sandia National Laboratories for designing and fabricating the microfluidic system used in the experiments. The system was developed with contributions from Conrad D. James, Matthew M. Moorman, Ronald P. Manginell, Jeffrey W. Lantz, Ronald F. Renzi, Jerry Inman, James L. Van de Vreugde, Daniel Porter, Carlton Brooks, Anthony Martino, and Anup K. Singh. Sandia is a multiprogram laboratory operated by Sandia Corporation, a Lockheed Martin Company, for the United States Department of Energy's National Nuclear Security Administration under Contract DE-AC04-94AL85000.

I have been fortunate to collaborate and interact with a very diverse, intelligent, and awesome group people in my graduate studies at UNM. I would like to thank the former and current members of the OWL (Janet Oliver, Bridget Wilson, and Diane Lidke) lab for the solid scientific foundation you created and the wealth of knowledge you constantly bring to the lab. Specifically this includes Dr. Chris Valley who was always there to be a sounding board and a guide for all my scientific problems. Emanuel Cavazos who was always there to be distracted by discussion scientific and nonscientific. Ellen Hatch who was not only there to theorize about scientific thoughts but was there for a workout partner. Samantha Schwartz who was constantly available to divulge and deliberate any scientific subject as well as help assimilate to the lab equipment and microscopes. Dr. Rebecca Lee for the creation of a very concrete experimental base from which to grow from. Dr. Avanika Mahajan for her continuous support in the experimental base and scientific progress as well as her friendship. I was always able to banter about science and non-science related subjects with Richard Pepermans. Dr. Keith Lidke had an impeccable way of teasing out the details of a problem and furnishing many solutions. Dr. Pat Cutler was not only there as a friend but to discuss MatLab script writing and scientific notions, his knowledge is invaluable. I owe my growing knowledge of the confocal microscope and biological concepts to Dr. Amanda Carroll-Portillo and Dr. Heather Ward. Dr. Shalini Low-Nam was a prime example of how I driven I thought I needed to be to complete my degree, an aspiration indeed. Jason Byars for his help in setting up the microfluidic device and constant intellectual input about computers and hardware. Guanghua Wan for her stylistic scientific input throughout my time in the lab. Annikka Jenson for not only her impeccable scientific eye but her continuous friendship. I want to thank Anna Holmes, Rachel Grattan, Carolyn Pehike, Genevieve Phillips, Mary Raymond Stintz, Dr. Ksenia

Matlawska-Wasowska, Anza Darehshouri, Angela Welford, Hanna Johnson, Peter Relich, Dr. Olena Ivashyna, Dr. Fang Huang, and Patrick Johnson for their collaboration, knowledge brought to my eyes, and friendship.

Calcium Signaling Dynamics in RBL cells under Pulsed Ligand Exposure

By

Mario J. Paz

B.S. Mechanical Engineering, University of New Mexico, 2006

M.S. Nanoscience and Microsystems Engineering, University of New Mexico, 2014

ABSTRACT

Understanding cellular signaling is important to learning about life at a fundamental level. As an extension of this, understanding the dysregulation of cell signaling is the key to identifying and treating disease. At present, there are multitudes of ways to investigate the cell signaling process, from immunofluorescence to single particle tracking. These techniques are advantageous in their own right, but having the ability to interrogate suspension and adherent cells with reagents at high temporal resolution and image them simultaneously is a process that could uncover many unseen signaling events.

In Aim 1, we describe a microfluidic device for live cell imaging of cell signaling events after ligand activation. This investigation method is able to capture early events with a high temporal resolution. When coupled with fluorescence microscopy the responses of single cells loaded in the device can be measured using fluorescent reporters. In Aim 2, we have measured with high temporal resolution the calcium response of mast cells exposed to stimulus. Cells labeled with the calcium indicator dye, Fluo-4, are loaded into the microfluidic traps. By monitoring the intensity of emitted fluorescence from the excited Fluo-4, the amount of intracellular calcium can be measured. When exposed to the stimulus, we observe a change in the fluorescence emission, indicating calcium flux upon ligand activation. This study focuses on the use of a microfluidic device supplied by Sandia National Laboratoriess to track the cytoplasmic calcium changes due to ligand addition for the FcεR1 pathway in Rat Basophilic Leukemia (RBL) cells. Specifically the investigation will look at stimulation pulses over a range of duration, and compare single stimulation pulses to multiple pulses in order to achieve a more in depth understanding this signaling pathway.

TABLE OF CONTENTS

CHAPTER 1: INTRODUCTION

1.1. FcεR1 Signaling

FcεRI signaling is central to the pathology of allergic responses. In the response, B-cells (Andrews, Lidke et al. 2008) are exposed to an antigen after which they produce antibody for this antigen, called IgE that has a high affinity for the FcεRI receptors on mast cells. The receptors on mast cells are increased in number and stabilized at the membrane surface after exposure to IgE, as seen in Figure 1 A. When these cells see the antigen again the FcεRI receptor aggregates due to the multivalent antigen, 2,4 Dinitrophenyl- Bovine serum albumin (DNP-BSA). This multivalent ligand that substitutes for natural allergens like cat dander or mold. This

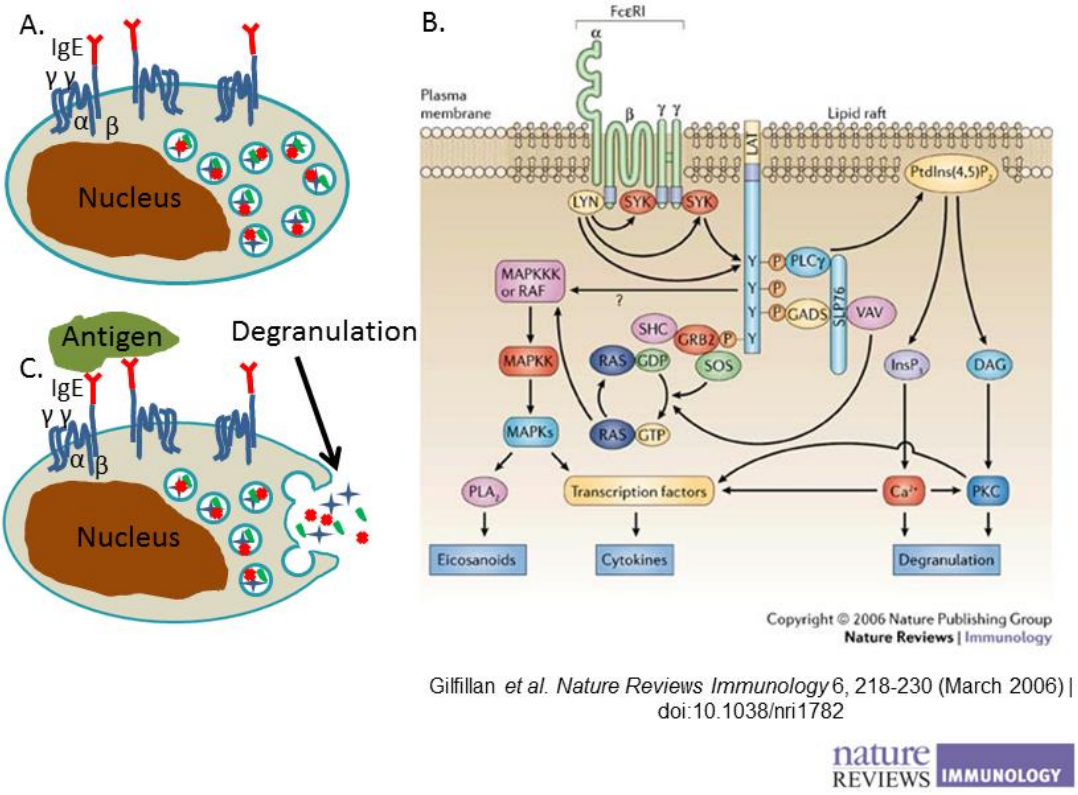

Gilfillan *et al. Nature Reviews Immunology* 6, 218-230 (March 2006) | doi:10.1038/nri1782

nature REVIEWS IMMUNOLOGY

Figure 1. FcεR1 signaling cascade diagram. Resting cells express the FcεR1 receptor, which contains the gamma, alpha, and beta protein chains, shown as blue lines at the cell surface. These cells have granules that are held within the cell, these are shown as the bubble shapes in the cell having red, blue, and green objects in them representing the histamines and other mediators of inflammation, which the cells hold naturally. A.) The receptors are primed with IgE, shown as a red "Y", which binds with high affinity to the alpha chain of the FcεR1 protein through its Fc region and recognizes the hapten DNP. DNP-BSA is uses as the antigen for the system. The IgE molecule stabilizes the receptors at the membrane and recruits more Fc receptors to the cell surface. B.) After addition of DNP-BSA, shown as the green mass, receptors aggregate initiating a cell signaling cascade event which in turn leads to a movement of proteins in the cytosol. The DNP-BSA molecule is multivalent with an average of 24 DNP/BSA and has the ability to bind to a multiple IgEs. C.) This eventually causes a movement of calcium from stores and degranulation of histamines.

causes downstream signaling events (Figure 1 C) and eventually degranulation of histamines and other mediators of inflammation (Mahajan, Barua et al. 2014), as seen in Figure 1 B.

1.2. Calcium as a Secondary Messenger

In downstream signaling events and before degranulation, calcium is used to affect other biological molecules. Calcium is a second messenger working across the body in a plethora of different cells. A change in calcium concentration can take place due to a variety of different reasons from mechanical stimulation o loading (Yang, Chen et al. 2009, Fowlkes, Wilson et al.

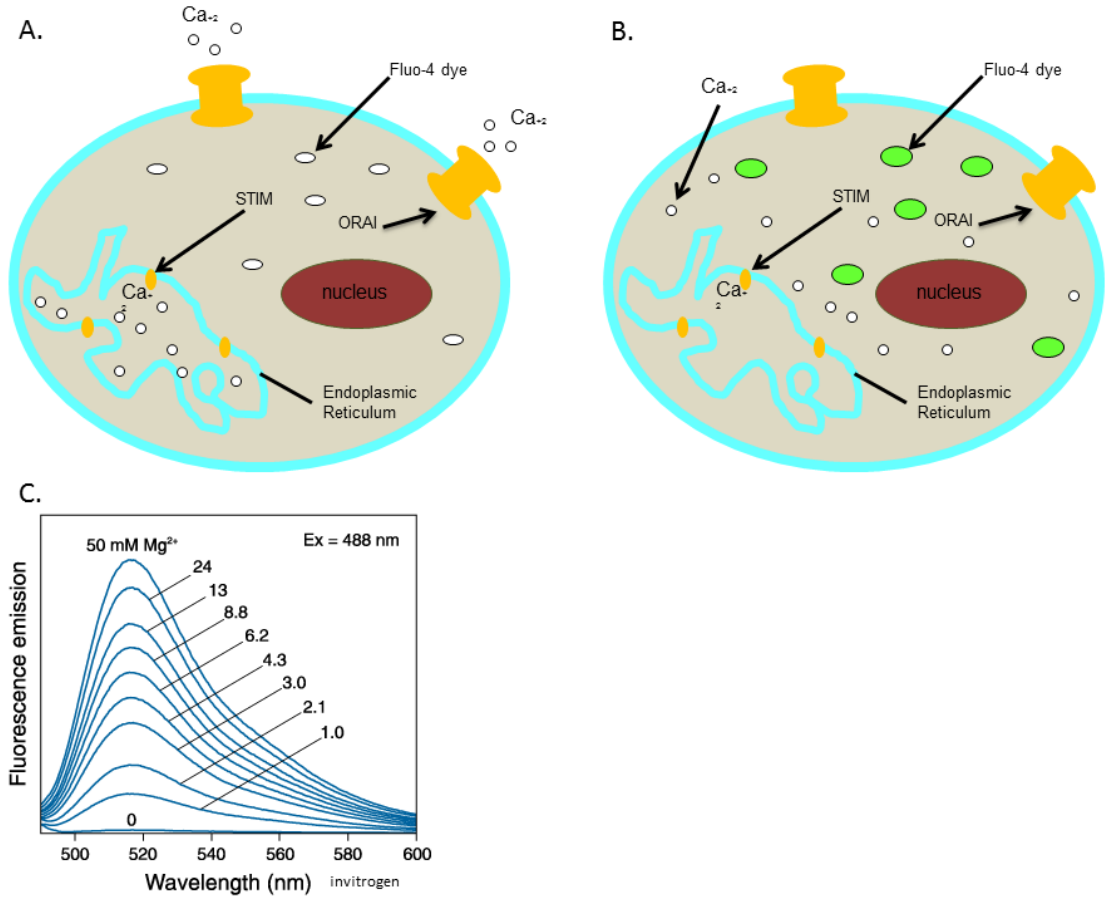

Figure 2.Tracking of calcium signaling. Since calcium is used as a secondary messenger it was important to develop a method to track its movement in the cell. The calcium indicator dye, Fluo-4, is loaded into the cytoplasm of RBL cells where the molecule then awaits a change in calcium concentration. A.) When the cell is in a resting state the unbound Fluo-4 dye molecule is in a dark state because of the lack of calcium in the cytoplasm. B.) After the cell is activated, calcium is moved into the cytoplasm from the cells calcium stores. The Fluo-4 molecule is then changed to a fluorescent state as the calcium bindings to it. This change can be monitored using fluorescence imaging. C.) The Fluo-4 fluorescence emission is directly related to the concentration of calcium. In the Invitrogen product curve shown here, Magnesium was tested, which has the same valiancy as calcium used as a secondary messenger in the cell. This makes it a substitute for testing fluorescence emission of Fluo-4.

2013) to apoptosis (Memon, Munk et al. 2011) to activation of membrane receptor complex's (Sanchez-Gonzalez 2010, Cefaliello, Eyman et al. 2014, Jayasinghe, Munro et al. 2014). Many questions can be investigated by tracking the movement of cytoplasmic calcium, from receptor signaling dynamics, either on the membrane (Gimborn, Lessmann et al. 2005) or on the endoplasmic reticulum (Chalmers, Schell et al. 2006) to adaptor proteins actuation (Silverman, Shoag et al. 2006) and in coordinate with another output such as degranulation in mast cells (Liu, Barua et al. 2013).

Since calcium is directly involved in the biology of many signaling cascades, tracking its movement would be very advantageous. Intracellular calcium concentration is monitored via an indicator dye. These dyes have an unbound calcium fluorescent state. In the case of Fluo-4 the unbound state is a dark state, which is shown in Figure 2 A. Then after ligand activation, intercellular calcium is released and binds to the dye which changes the fluorescence state of the molecule. The Fura-2 molecule changes fluorescent excitation states, while Fluo-4 is brought to a fluorescent state, as shown in Figure 2 B. Additionally, the dark state to fluorescent state shifting dyes need dye concentration calibration in order to keep away from saturating the camera pixels while imaging. The dye is cell membrane permeable and kept intracellular by its attached acetoxymethyl ester. Also in the case of Fluo-4, the dyes intensity is directly proportional to the concentration of intercellular calcium as shown in Figure 2 C (Gee, Brown et al. 2000).

The use of calcium indicator dyes as a cytoplasmic calcium concentration monitor has led to many important discoveries. One example is the link between mitochondrial calcium flux and mast cell degranulation (Suzuki, Yoshimaru et al. 2006). In this study it was further found that the mitochondrial permeability transition pore (mPTP) is involved with the regulation of calcium and degranulation. Namely it enables the mitochondria to act as a fast calcium release store and that mPTP negatively regulates the calcium release from extracellular stores. A second interesting finding by calcium investigation is the connection between Fyn and the calcium stores being elucidated (Tshori and Razin 2010). It was found by Tshori et al. that in certain mast cell phenotypes the transient receptor potential cation channels (TRPCs) can be opened by Fyn kinase to cause calcium influx rather than through the activation of the STIM-ORAI channels. Yet another calcium signaling study by Cohen et al. found mast cells to produce calcium waves

initiated by a treatment with soluble antigen, which is presented as a very controllable process. Moreover the stimulation is able to be on a specific spot or on the cell holistically (Cohen, Torres et al. 2009). Using another cellular stimulation method, it was found that external calcium waves on a cell causes an antigen stimulated calcium response in mast cells (Lee and Oliver 1995). Rebecca Lee and Janet Oliver furthermore show that the extracellular calcium modulates calcium stores release via an antigen-induced influx of calcium. Another study explored the exploitation of multiple roles of PI3-kinase in the mobilization of calcium in activated mast cells (Barker, Lujan et al. 1999). In Barker et al., it was found the two isoforms of PLCγ are both activated by PtdIns-(3,4,5)-P3 independent of the phosphorylation state of the two enzymes. Furthermore, data in the study suggested that the basal tyrosine phosphatase activity holds the FcεR1 pathway in balance with cross-linker absent.

1.3. Investigation by Microfluidic Device

Since the above mentioned findings could be discovered with minimal control over key factors in experiments, more control over the extracellular environment could offer more information to be uncovered. The ability to control a cell's surroundings can be an important tool for investigating cellular responses, and furthermore has applicability in examining cells' calcium signaling dynamics. More specifically, changing a cell's environment on a very short timescale and being able to measure a signaling response due to that change will increase understanding of how the cell responds to stimuli. As an extension of this, determining what happens in protein-protein interactions during a mutation, which perturbs the signaling of the system, has the ability to uncover some of the mysteries in pathology.

One way of achieving this kind of control is through the use of microfluidic devices. Microfluidic devices have paved the way for the investigation of biological molecules using small volumes of liquid with complete control of the cellular surroundings (Muzzey and van Oudenaarden 2009). Applications of these devices for cellular systems involving bio molecules have led to studies in electrophoretic immunoassays (Shackman, Dahlgren et al. 2005), impedance spectroscopy (Han and Frazier 2006) (James, Reuel et al. 2008), optical microscopy (Wheeler, Throndset et al. 2003), (Tourovskaia, Figueroa-Masot et al. 2005), (Di Carlo and Lee

2006) and electrochemical detection (Amatore, Arbault et al. 2007). Microfluidics technology has also been extended to study cellular response to an activating or stimulating molecule, (Mettetal, Muzzey et al. 2008) (Hersen, McClean et al. 2008). This was done, for instance, by capturing the dynamics of the Hog1 MAP kinase cascade during hyperosmotic changes to budding yeast and evaluating the shock response. Also microfluidics has been used to see cellular changes of endothelial cells due to a change in the cells immediate environment (Whitesides, Ostuni et al. 2001).

Along with changing the cell's immediate environment, microfluidics allows for controlled environments for whole specimens for fully in vivo studies (Zhao, Xu et al. 2013) and for cell culture monitoring in order to probe for cell metabolism (Weltin, Slotwinski et al. 2014), as well as customizing cell culture conditions (Gomez-Sjoeberg, Leyrat et al. 2007). This makes answering questions on any level of systems biology more tractable when dealing with a controlled volume that can be changed due to the problem or angle on the problem needing to be answered (Szallasi, J et al. 2006). Microfluidics also provides the capability to design a multitude of different architectures that exploit properties from those designs to answer a biology problem. Such designs include Dean vortex flows present in curvilinear microchannels that are used to sort cancer cells on chip (Warkiani, Guan et al. 2014), and the use of laminar flow in microchannels to sort cells or particles for reactions, analyses, and labeling (Tarn, Lopez-Martinez et al. 2014). Some of the biological applications that can be captured include cell adhesion studies (Hartmann et. al, 2014), glycolytic oscillations of yeast cells (Gustavsson, van Niekerk et al. 2014), and microfabrication of human organs on chip (Huh, Kim et al. 2013). Also, recent advances in bioluminescence and chemical luminescence allow for detection of cellular events on microfluidic platform (Mirasoli, Guardigli et al. 2014). With the use of these techniques biological processes can be viewed in real time. This paves the way for visualization of cell signaling events by epifluorescence (Sawano, Takayama et al. 2002).

The need for development of a microfluidic device with a unique architecture for the capture of single cells, as well as providing strict control of reagent delivery to the cells guided the device design used for this study. The chip was designed to allow fast reagent switching, as there are two entrance ports flowing into a shared channel with an exact flow separation. As the fluids in the device are pressure driven, a change in inlet pressure differential causes immediate

movement of fluid in the shared channel, therefore bringing reagent adjacent to or away from the traps, due to an increase or reduction in the pressure differential, respectively. The chip is sealed with a glass coverslip, which allows for high-resolution microscopy and other optical investigation techniques. The system is designed to facilitate the high temporal resolution of reagent delivery to the traps and assure homeostasis in the cells being investigated due to temperatures staying physically relevant. Reagent delivery is provided by the use of pressure regulators, which manage pressures from 0-15psi. The pressure placed on the systems entrance ports is directly related to the position of the flow separation in the shared channel. Having temperature controllers on the reservoirs and the manifold ensure the temperatures of the all fluids used are at biological temperatures.

1.4. Specific Aims

Aim 1: Characterize a microfluidics device for rapid delivery of stimulus.

The previous findings showcased above have given some depth to the field of microfluidics. It is good to point out some of the studies specifically to get a sense of what inspired the current work from the literature. Muzzey and van Oudenaarden's study showed you could have control over the microfluidic environment. Also Hersen, McClean et al. and Mettetal, Muzzey et al. showed application of microfluidics to the study of cellular response could be done. Szallasi et al. showed that you could easily change the device design for a problem needing to be studied. Swano et al. showed that investigation of biological process could be down in real time with epifluorescence. We decided to fuse some of the above ideas and to build a microfluidic device, which gives the ability to image live cells in a controlled environment. This particular device has the ability to trap cells, whether they be in suspension or adherent and add something that challenges or activates the cells. And furthermore this device has the ability for a high time resolution of reagent presence at the cells.

Aim2: Measure with high temporal resolution the calcium response of cells exposed to stimulus.

Previous work in FcεR1 calcium signaling has shown progress in a few areas. Generally it was discovered that receptor signaling dynamics of membrane proteins, ER proteins, and adaptor proteins can be tracked by calcium changes in the cytoplasm. But, there are also many other things that can be investigated in this signaling pathway. We feature experiments that will investigate the FcεR1 pathway changes using different stimulation points, by tracking the changes of calcium in the cytoplasm. For this study, we noted the need of microfluidics to accomplish the task of having shorter stimulation points of antigen. Typically, researchers stimulate cells by addition of antigen in a single bolus, such that once added it cannot be easily removed. It has been shown in past studies several problems elucidated using this method. But with the ability for shorter time points more questions can be posed. One question never asked is how would the FcεR1 system react to a smaller time of ligand stimulation? How would that compare to longer stimulation? What is the effect of repeated stimulation points? Is there a way to determine the systems bandwidth, which is the range of frequencies that transmit signal? Moreover what would this frequency stimulation time be in design? And would it be a single stimulation or multiple stimulations? In order to answer these questions microfluidics is an advantageous science to incorporate. With the help of this science cellular responses have been studied already, with epifluorescence. It would be a matter of designing a chip to answer the questions listed above. To reiterate, the overall goal of this study would be to have a system which could house cells, investigate calcium signaling due to activation of the FcεR1 protein.

To accomplish these aims, several types of experiments were performed. First, experiments performed on coverslip were conducted with the antigen (DNP-BSA) added to activate the cells and ionophore to test the cells' viability. These gave indication on the studies relevancy to the literature. Next experiments were done on adherent cells in the microfluidic device channel. Three experiments were carried out, one to test basophile activity to a directed stream across the cell, and this is called microfluidic channel shear flow. The next two experiments were similar to the coverslip experiments, addition of DNP-BSA and ionophore. These experiments tested the environment in the device and compared responses in the device to those obtained from coverslip experiments. Next, two control experiments will be done in the trap area. The first is a positive control and the cells were given buffer containing antigen for an infinite amount of time. This sampled the higher end of activation we saw. The second is a negative control; the cells were given buffer only. This tested the shear flow activation of the

cells to gather the baseline activity of the cells in the device. Finally, experiments in the traps were conducted by lowering the time in which the cells are exposed to ligand, to compare long-term stimulation versus short-term and single pulse versus multiple pulses.

CHAPTER 2: MATERIALS AND METHODS

2.1 Device fabrication and design

The microfluidic device and control hardware was fabricated by our partners at Sandia National Laboratories. Microfluidic channels were fabricated in silicon wafers using deep reactive ion etching and devices were later sealed with glass coverslips using anodic bonding. Here, the cell trap design was modified to include multiple levels of etching in the microfluidic channels in order to constrain cells near the coverslip surface for optimal imaging. The microfluidic chips were interfaced to a manifold and fluid delivery was controlled with a set of electronic pressure controllers and electronic microfluidic valves (Anup K Singh 2009, James, Moorman et al. 2009)

2.2 Experimental Set Up and Procedures

For microfluidic device experiments the chip and manifold were used. The manifold was mounted to an Olympus iX71 inverted microscope and devices were first purged with degassed ethanol, and degassed deionized water using the pressurized system, then Hanks media was flushed in the chip to passivate the chip surfaces. RBL-2H3 cells were loaded with 2.5 µM Fluo-4 at 37^{o} C for 20 minutes and placed in an aliquot tube for use on the device. Cells were then introduced into the device placing the aliquot tube on the reagent reservoir stand and loaded onto the device for experiments.

The microfluidic coverglass experiments were done by loading RBL cells into the device and brought to the channel area between inlet 6/5 and 8/3. They were left to settle and attach to the glass. Then, either 1) Hanks buffer and Texas Red-BSA, 2) Hanks buffer and 1µg/mL DNP-BSA plus Texas Red-BSA, or 3) Hanks buffer and ionophore (A23187 at 1µM Sigma, C5149) plus Texas Red-BSA, were brought to the cells. For the trap area microfluidic device experiments, cells were brought into the device and caught in the trap region. The cells were then exposed to either Hanks buffer and Texas Red-BSA or Hanks buffer and 1 µg/mL DNP-BSA

plus Texas Red-BSA to get a response after being trapped. Texas Red was added to the Hank's buffer at a concentration of 76 nM (Molecular Probes A23017) to visualize the pulse stream.

For 8 well chamber experiments 40,000 cells were seeded per well and kept in MEM media overnight. Cells were then loaded with Fluo-4 for 20 minutes at 37 ^{o}C. Cells were then imaged on the microscope stage.

The microscope contains a filter cube with an excitation filter that passes 479 and 585 nm wavelength light, a beam splitter at 505 and 606 nm and an emission filter at 524 and 628 nm for simultaneous imaging the Fluo-4 and DNP-BSA (Invitrogen, molecular probes, A23018, 1 µg/mL concentration) with BSA-Texas-Red solution, respectively. Images were taken using an AndorIxon CCD camera and analyzed in Matlab.

2.3 Cell and Sample Preparation

Rat Basophil Leukemia cells RBL-2H3 were grown in Ultra Low 100 dishes so they stay in suspension, then were primed with DNP-specific IgE (Liu, Barua et al. 2013) at a concentration of 1µg/mL for overnight or 3 µg/mL for 2 hours. For microfluidic device experiments on the day of experiments, the cells used were passed through a 40 µm nylon mesh filter (Falcon, 352340) to remove cell aggregates and noncellular debris. After that the cells were loaded with Fluo-4 at a concentration of 2.5 µM (Invitrogen, molecular probes, F14201), to track the movement of calcium in the cell.

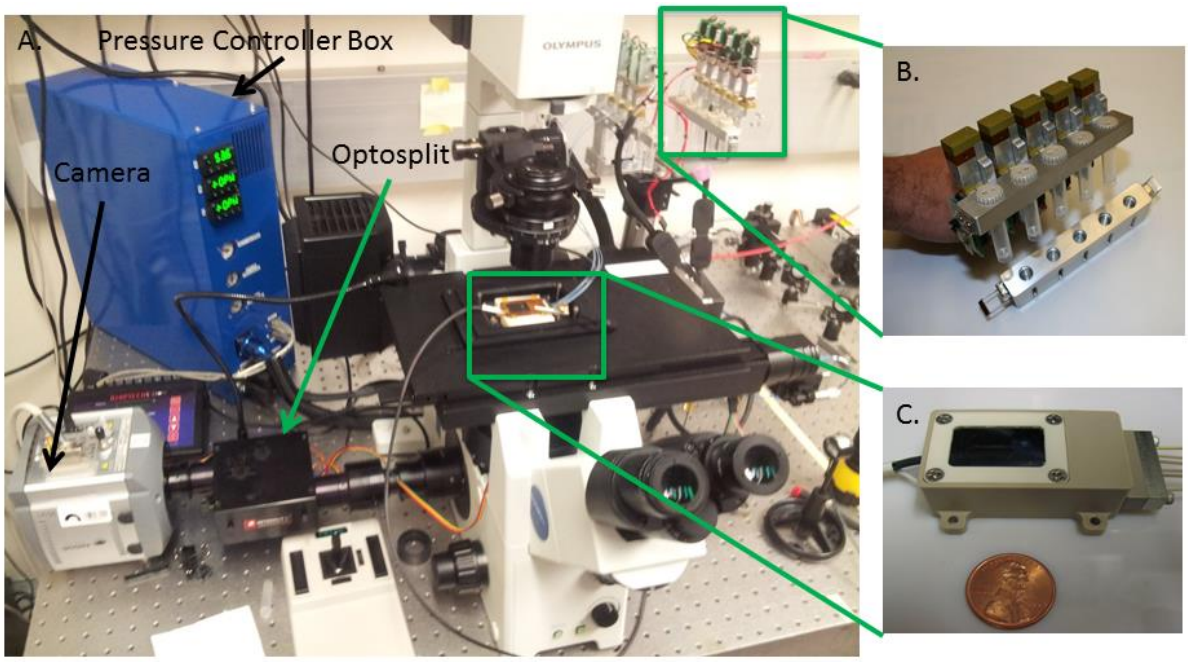

Figure 3. Overview of microfluidics system. A) The microfluidic manifold, indicated by the green box, is mounted on an iX71 Olympus inverted microscope fitted with an Optosplit dual view image splitter, and Andor iXon emCCD camera. The pressure controller box controls the pressure that drives the flow through the microfluidics device. B) Reagent reservoirs, indicated by the green box in the larger screen shot, are coupled to individual inputs or output on the manifold. C) The manifold consists of a microfluidic chip (black region) that is mounted by the manifold frame that provides connections (right side) for the tubes coming from the reservoirs.

CHAPTER 3: RESULTS

3.1. Microfluidic Technology

Calcium signaling of FcεR1 has previously been done in eight well chambers on adherent cells. This methodology makes it difficult to investigate the amount of antigen stimulation needed for cells to respond and whether that is an additive or holistic effect. The development of an investigation method was necessary to view events of this nature. Technology, which is capable of investigating such events, is shown in Figure 3 (Figure 3 A). In this image the microscope used for the study is shown, as well as the pressure and temperature regulation box used for pressure and temperature regulation of the system. The reagent reservoir stands (Figure 3 B) and the manifold, which sits on the stage of the microscope, are also illustrated (Figure 3 C).

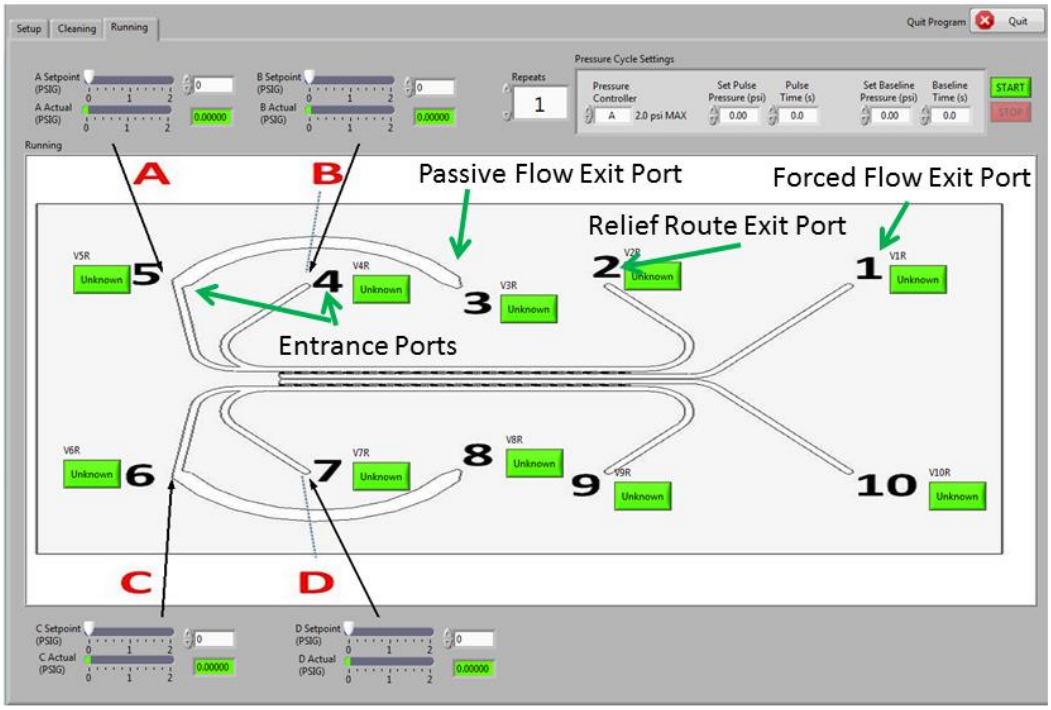

Figure 4. Chip layout and Graphical User Interface (GUI). GUI shows the chip layout, with entrance ports (5/6 and 4/7), all the way to the left of the schematic. The passive flow exit port (3/8) is just to the right of the entrance ports. The relief route exit port (2/9), further to the right, is where fluid flows by the trap area. , The forced flow exit port (1/10), furthest right, where fluid is forced across the trap area. Pressure is regulated at the entrance ports and flow is directed in the path of least resistance from the entrance ports toward any exit port opened. The GUI is used by clicking on the green button, in the program, to open or close the valve associated with that button. The set point is set to a desired pressure setting to get fluid moving in the direction of one or more exit ports opened. At the top of the GUI the user can set a particular pulse quantity, pressure, and time can be set in order to facilitate repeated pulse experiments easily.

This system is controlled by the graphical user input (GUI) (Figure 4), which also shows the layout of the chip. Each chip has the ability for two experiments to run two experiments side by side, on ports 1-5 or 6-10, with entrance of fluid on chip from 4/6 and 5/7 by application of pressure at those ports. Exit ports are at 3/8, 2/9, and 1/10. Exit ports 1 and 10 are considered the forced flow because when only that exit is open, the flow is forced through the traps to the exit port. The exit ports 9 and 2 are called the relief flow because the flow goes past the traps to the exit. The exit ports 1 and 10 are called the passive exit ports due to liquid not flowing towards the traps at all. To exemplify how the boundary of the flow in the device is changed and the time scale upon which it changes, an experiment was done with water and fluorescent food coloring flowing in entrance port 4 and water flowing in entrance port 5, with both flowing out exit port 2 (relief route) (Figure 5 A). At the beginning of the experiment both entrance port pressures were set at 0.6 psi. The entrance port 5 was decreased to 0.5 psi, which moved the stream boundary towards the traps and brought the fluorescent food coloring in deionized water in stream 4 to the

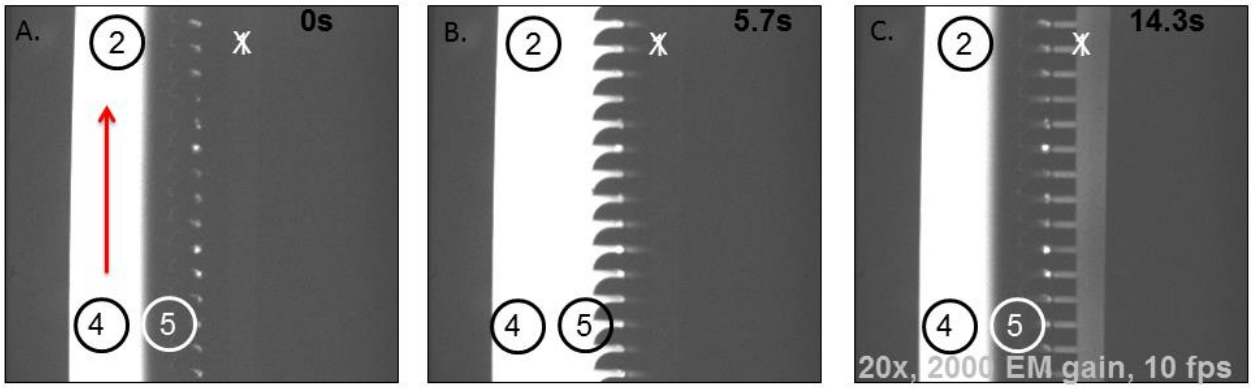

Figure 5. Initial ligand pulse experiment. These images are taken from a time course during a pulse experiment. A) Fluorescent food coloring (white) in deionized water and deionized water (black) were brought into the device through inlet 4 and 5, respectively. Keep in mind throughout the experiment the forced flow outlet (outlet 1) was kept closed. The pressure at inlet 4 and 5 were both set to 0.6 psi at the beginning of the experiment. B.) Next at 5.7 seconds, the pressure at inlet 5 was changed to 0.5 psi and the pressure at inlet 4 was kept at 0.6 psi. This causes the fluorescent stream (white) to overtake the non-fluorescent stream (black). C.) Finally at 14.3 seconds, the pressure at inlet 4 and 5 were both brought to 0.7 psi. This intern brought the fluorescent stream (white) back away from the trap structures and overtake the non-fluorescent (black) stream.

traps in 5.7 seconds (Figure 5 B). Then a few seconds later the pressures of each inlet were set at the same 0.7 psi pressure setting. This brought the stream boundary away from the trap area by 14.7 seconds (Figure 5 C). By virtue of a difference in pressure of the inlet settings the boundary of the streams is able to be moved to or away from the tap area.

Now that the fluid exchange has been discussed, the next thing to explain is how cells were loaded into the device. After preparing the device for biologicals, cells were brought into 6/5 and out 8/3, and when a good density of cells was seen by eye, through the microscope

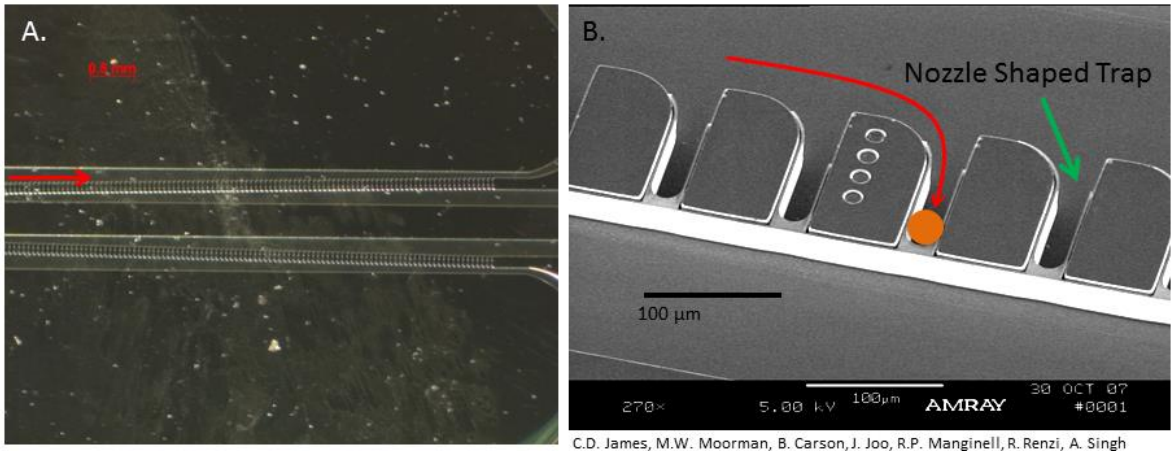

Figure 6. Trap area overview. A.) A closer view of the chip shows the trap area, specifically how they are laid out in a staggered manner from the entrance (red arrow) to the exit of the trap area. B.) A closer view of the trap area displays individual nozzle shape structures (green arrow) lined up side by side. Cells (orange dot) are trapped by first flowing cells into the device, past the trap region, and out the relief route. When ready the cells are taken into the nozzles (red arrow) by opening up the forced flow across the traps. Cells will populate the trap region one in each nozzle. Once a cell is present in a nozzle that particular nozzle is less likely to attract another cell.

ocular, the user opened exit port 9/2 and closed port 8/3. This changed the flow of cells toward exit 9 (2) as well as toward the traps (Figure 6 A). Then the cells were trapped by opening the forced flow and cells were brought into the traps (Figure 6 B). Once an individual trap had a resident cell, that particular trap was less likely for another cell to take residence in it. After loading cells into the device, then they are activated with ligand. In order to display the diverse pulse designs that can be created with the microfluidic system, different pulse widths and pulse trains were conducted. The first carried out was a 25 second single pulse (Figure 7 A). This pulse width was also used in experiments. The second pulse width tried was a five second pulse (Figure 7 B). This pulse width tested the time resolution of the microfluidic system as it was the shortest pulse width. The next two pulse widths, 50 seconds and 2 minutes and 5 seconds, showed how the system functions with larger pulse widths (Figure 7 C and D). Next a pulse train was created with the pulse width being 5 seconds and a break time of 55 seconds (Figure 7 E). This tested the shortest cycle time that could be conducted with the system. Finally a 25 second pulse train was conducted with the system. This was a design with a 25 second pulse width and 95 seconds between pulses (Figure 7 F). This pulse train experiment was also very close to the

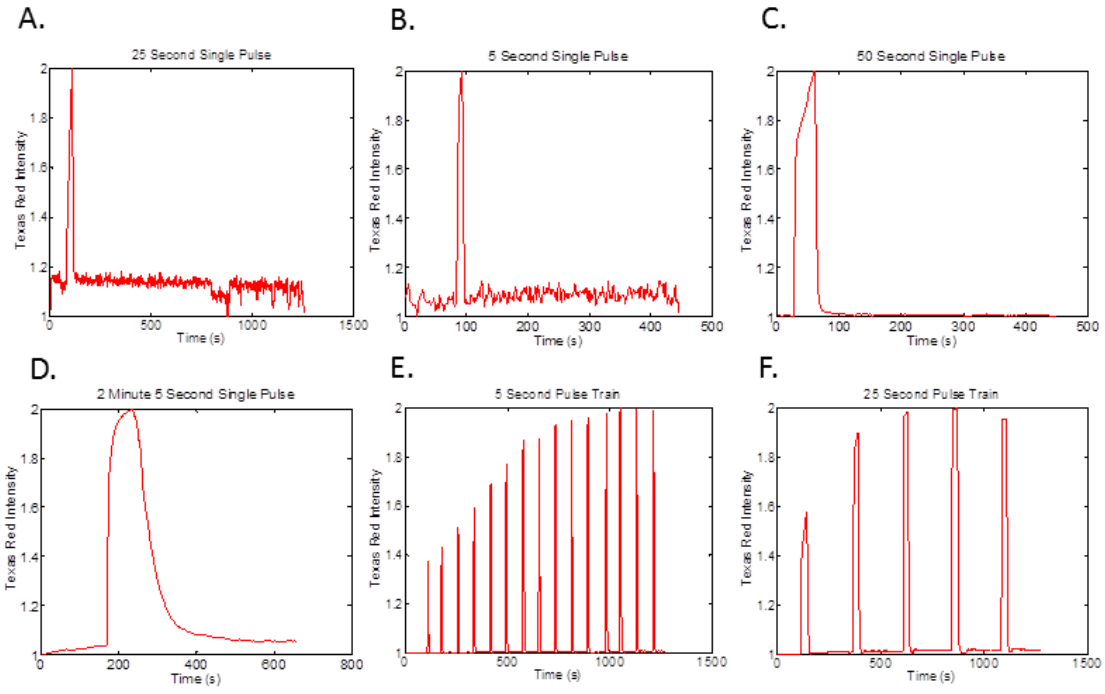

Figure 7. The variety of pulse width and pulse train experiments. There are a vast amount of reagent pulse widths which are able to be created by the microfluidic system. A.) To show some of the pulse widths that can be created, first a 25 second pulse experiment was done. This is the pulse width used in experiments. B.) Secondly, a 5 second pulse experiment was conducted. This pulse width was about the shortest pulse width that could be one with the system. C.) and D.) Next, a 50 second pulse and 2 minute and 5 second pulse width was carried out. This showed the larger pulse widths the user could actuate. E.) For a different brand of experiment, 5 second pulse train was created with the system. The pulse train was created with a break 55 seconds between pulses and a pulse width of 5 seconds. This showed the shortest cycle time and pulse width conducted with the system. F.) Lastly, the 25 second pulse train is shown. This pulse train was conducted with a spacing of 95 seconds between pulses and a pulse width of 25 seconds. This is the pulse train that is used in the device list of experiments.

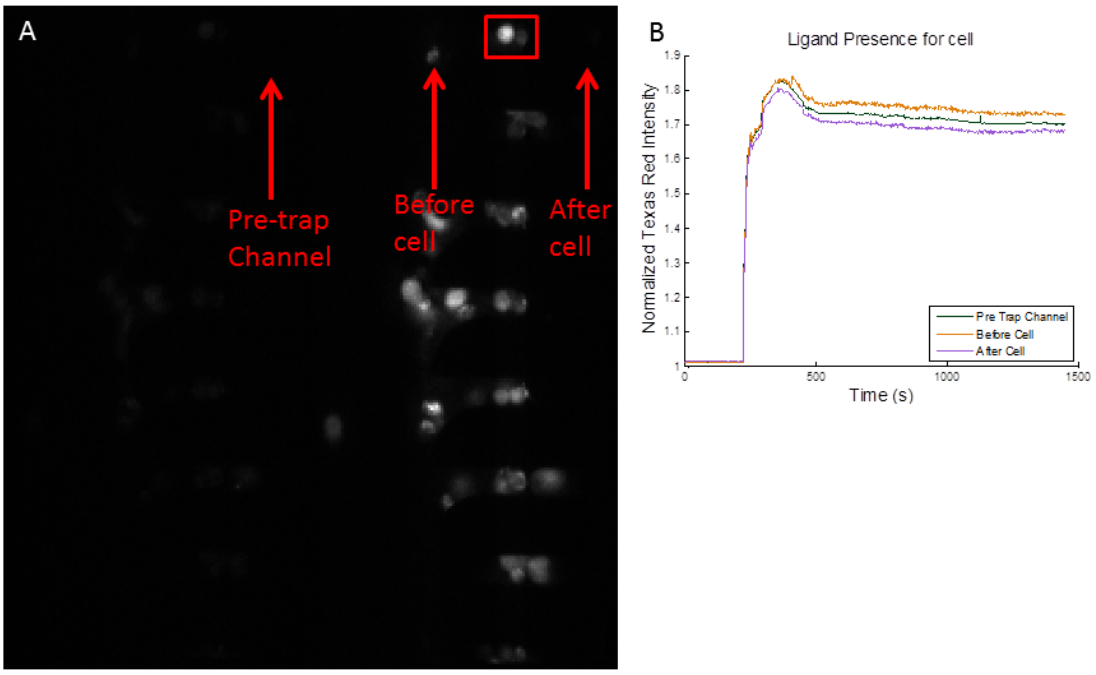

Figure 8. Ligand concentration at different locations in the trap region. A.) To test the distribution of ligand in the trap region three areas in the texas red channel were chosen and cropped per cell (red box). These areas namely are located in the channel before flow hits the traps (Pre-trap channel), before the flow hits the cell (before cell), and after the ligand hits the cells (after cell). B.) The Texas Red signal was analyzed from the three regions by first averaging the signal taken from one of the cropped regions in each frame of the sequence. Next the signal was normalized. This process was repeated for the three regions indicated. These data then were plotted against each other. The plots are placed very close together which indicates a uniformly distributed ligand concentration in the trap region.

pulse design used in the microfluidic device experiments.

After discovering the different types of pulse width and pulse train experiments that can be conducted, the ligand concentration was tested at a couple spots in the device. This test was done to get a sense of the variability of ligand concentrations across the trap area. The ligand concentration was tested namely in the region before the ligand would reach the cells (pre-trap channel), in the nozzle before the ligand could reach the cell (before cell) and after the ligand gets to the cell (after cell) (Figure 8 A). Crops were taken from each of these regions and the average fluorescence calculated for each frame in the three cropped sequences. These averaged values were normalized to the first ten points and plotted next to each other (Figure 8 B).

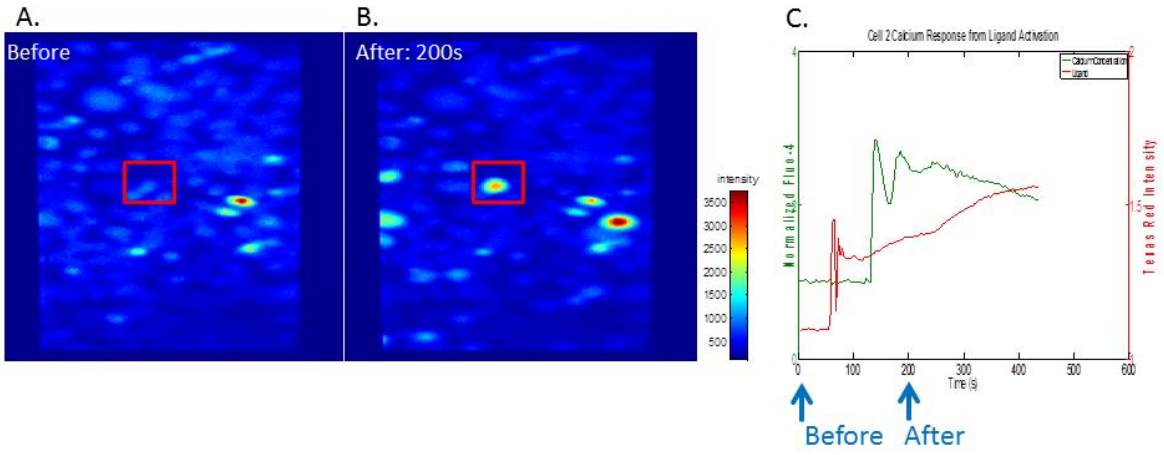

Figure 9. Example coverslip control experiment. A.) RBL cells were grown on a coverslip and labeled with Fluo-4. At 0 seconds the image is displayed from a sequence of images and one cell was highlighted (red box). The cells are resting at this time point. B.) Then 200 seconds into the experiment and after DNP-BSA is added, an image is displayed from the sequence of images. You can clearly see the difference in activity of the highlighted cell (red box). C.) This is shown graphically as the DNP-BSA (red line) increases shortly after the calcium response (green line) increases over time. The blue arrows denote time points highlighted in A & B (0 seconds and 200 second time points).

3.2 Control and Microfluidic Experiment Overview

The first calcium experiments were done on coverslip as shown in Figure 9. Figure 9 A shows an image of the Fluo-4 fluorescence at the start of the experiment and Figure 9 B shows an image of the Fluo-4 fluorescence 200 seconds into the experiment. Both of these images are taken in color map image scaling which shows the images intensity with a color reading. In this type of image red is more intense and blue is less intense. As you can see by eye, the same cell highlighted in both images shows a significant change in the color reading, indicating an increase in fluorescence of the cell and, therefore, the increase in calcium concentration in the cytoplasm of the said cell. This is shown graphically (Figure 9 C) as the cellular response is graphed (green trace) against the ligand addition (red trace) C.

An example of a pulse experiment with cells loaded in the microfluidics device is shown in Figure 10 A. Cells loaded with Fluo-4 have been deposited in the trap area and an image before (left), during (center), and after (right) the ligand pulse is displayed. The same cells are brighter in the image after the ligand pulse when compared to the before ligand pulse image. The same experiment is shown using a thermal gradient scale (Figure 10 B), where blue is lower intensities and red signifies higher intensities. The after image (right) shows more yellow and red areas than in the before image (left) which indicates an overall increase of Fluo-4 fluorescence.

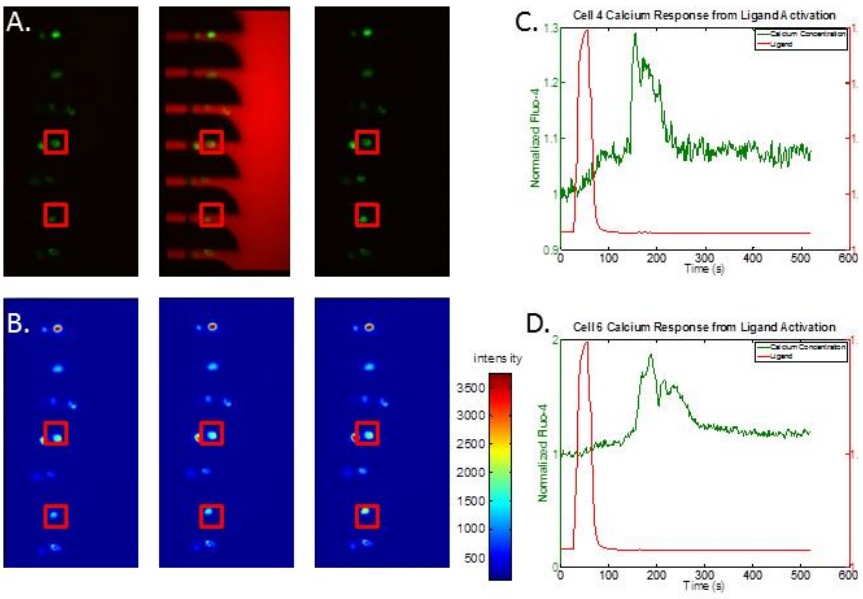

Figure 10. Microfluidic experiment images. A) RGB pseudo colored images were taken from a microfluidic device experiment, where the device was primed for biologicals then cells were loaded in the trap region (top left). Next ligand was brought to the cells to activate them (top center). After the cells are activated (top right) the movement of calcium and therefor activation of the cells is shown. The activation is observed by the relative brightness of the cells in the field of view compared to before the ligand pulse. B) Corresponding images are shown before (bottom left), during (bottom middle) and after (bottom right) of only the Fluo-4 channel. These images are shown in enhanced color map image scaling which puts emphasis on intensity changes that correspond to the change in Fluo-4. The change in Fluo-4 directly correlates to the movement of calcium within the cell. What is shown from this image styling is an increase in calcium within trapped cells. This increase in fluo-4 is shown from the overall increase in the red area within the field of view from the before to after time point. C. and D.) Two cell responses are plotted with the ligand exposure versus time (cell 4 and 6, respectively). Both cells show a spiked response shortly after ligand exposure.

The responses and ligand pulses are shown from two cells in this experiment. The first cell plotted is cell 4, (top red box) which was caught in the center of the field of view in the RBG and color map images (Figure 10 C). The second cell plotted is cell 6, (bottom red box) which is in the lower part of the field of view in the RBG and color map images (Figure 10 A).

3.3 Data Analysis

To analyze data more efficiently a GUI was designed to give the user the ability to batch analyze a number of experiment sequences (Figure 11). To load sequences the “browse” button was used to identify sequences that are to be batch analysis. The user then would click the “select” button in the GUI to choose the regions of interest (ROI) that will be used in analysis. The Texas Red-BSA channel is cropped first and then the Fluo-4 channel is second to be cropped. It is up to the user to define the number of Fluo-4 ROIs taken per Texas Red-BSA ROI,

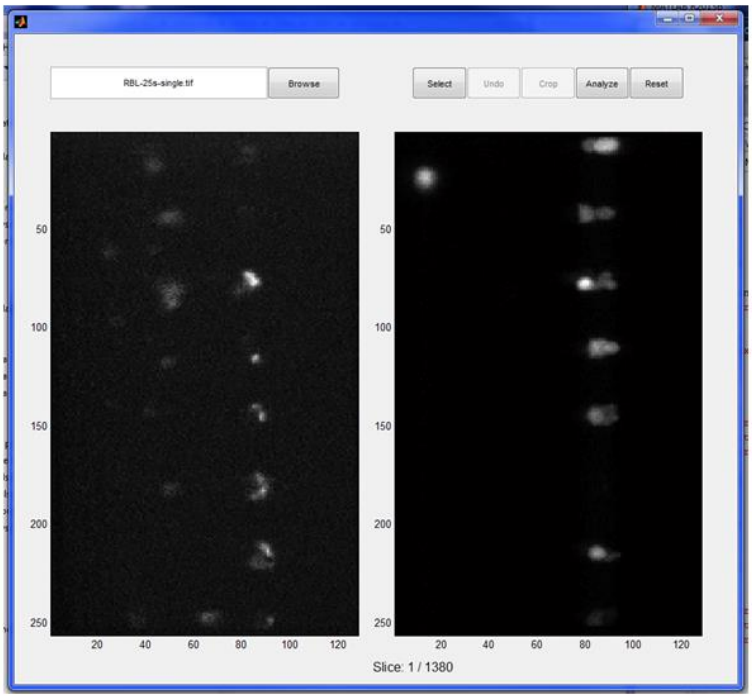

Figure 11. Screen shot of analysis graphics user interface (GUI). The GUI is able to load a number of experiment sequences to batch analyze, by using the "browse" button to identify each sequence. The user then presses the "select" button to start the cropping process. The Texas Red-BSA channel (left) should be cropped first and the Fluo-4 channel (right), second. One Texas Red channel (ligand) is cropped for as many Fluo-4 (cell) crops made. The user can undo a crop with the "undo" button. After all crops are made for all experiments the user presses "analyze" to manipulate and output the crops in a plotted form. The "reset" button resets the GUI the state it was in just after it was opened.

accounting for all of the cells captured in the field of view of the sequence. The user can undo a ROI by the "undo" button. After all the ROIs were defined the "analyze" button was used to analyze all the ROIs taken from all sequences. The "reset" button was used to reset all of the functions and settings in the GUI to the point of its initial opening.

After data collection, these data sets were analyzed by cropping the region over the cells in the Texas Red channel then averaging the fluorescence in each ROI of the frame, to give information about the ligand addition to the cells (Figure 12 A). Secondly, each cell was cropped out (Figure 12 B) and an average fluorescence was taken of the masked region within the cropped sequence of images (Figure 12 C). The average fluorescence from the Texas Red-BSA and Fluo-4 sequences was then normalized to the average of the first ten values in the plot. They were finally plotted against each other to show the calcium response from ligand addition (Figure 12 D).

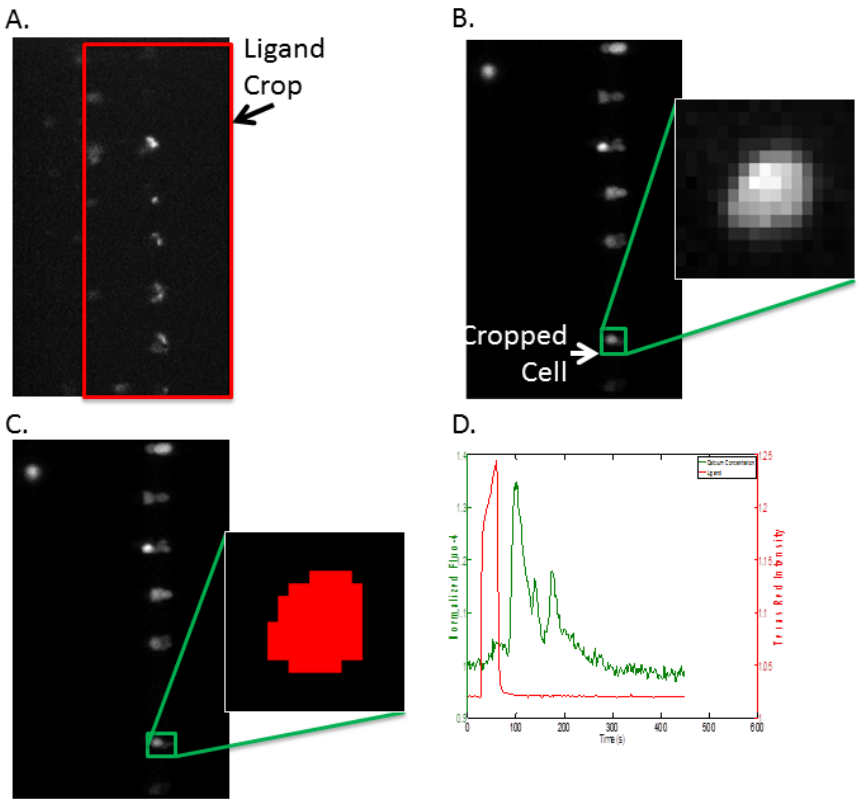

Figure12. Data analysis method. Using the Matlab interface, the ligand channel and the Fluo-4 channel are separated from the original sequence taken during the experiment. A.) Next, a crop is taken for the ligand channel (red box). This crop exists for each frame in the Texas Red sequence and the signal is averaged in each frame. This average signal is normalized and compared to each cellular response within one experiment. B.) Then, each cell is cropped from the Fluo-4 channel (green box) individually. C.) The cell is masked throughout the sequence to alleviate unwanted background. The signal within the mask for each frame is averaged and then normalized to the first ten frames. D.) Finally both averaged and normalized values are plotted side by side.

3.4. Microfluidic Experiment Overview and Parameters Logged

The initial experiments that were done with cells loaded in the trap region of the device were a positive (Figure 13 A and C) and negative control (Figure 13 B and D), doing an infinity pulse with and without ligand, respectively. There was a difference between having ligand and not having ligand in the pulse stream, as we expected. A couple of responses were shown in the positive controls, one in which there is a somewhat oscillatory effect in calcium concentration and then another with a large initial difference in calcium concentration after ligand addition that remained unchanged throughout the experiment. At the end of the experiment these responses

end up with the same effect, a stable increase in activation of the analyzed cell. These two responses are indicative of what was generally seen throughout these experiments, wholistically.

In this study five key experiments was conducted, using the microfluidic devices ligand delivery system. First of which was the 5 second single pulse width. This experiment showed no response from cells due to ligand exposure. This was also the shortest ligand pulse able to be created (Figure 14 A). The second was a 5 second pulse train (Figure 14 B), which had a 5 second pulse width repeated with a break of 55 seconds between pulses. This tested the temporal resolution of the reagent delivery to the cells, but showed no responses from cells. Next a 25 second single pulse experiment was conducted (Figure 14 C). This showed a response from a population of cells. Then a 25 second pulse train was created with a pulse width of 25 seconds and a break of 35 seconds between pulses (Figure 14 D). This experiment also showed a

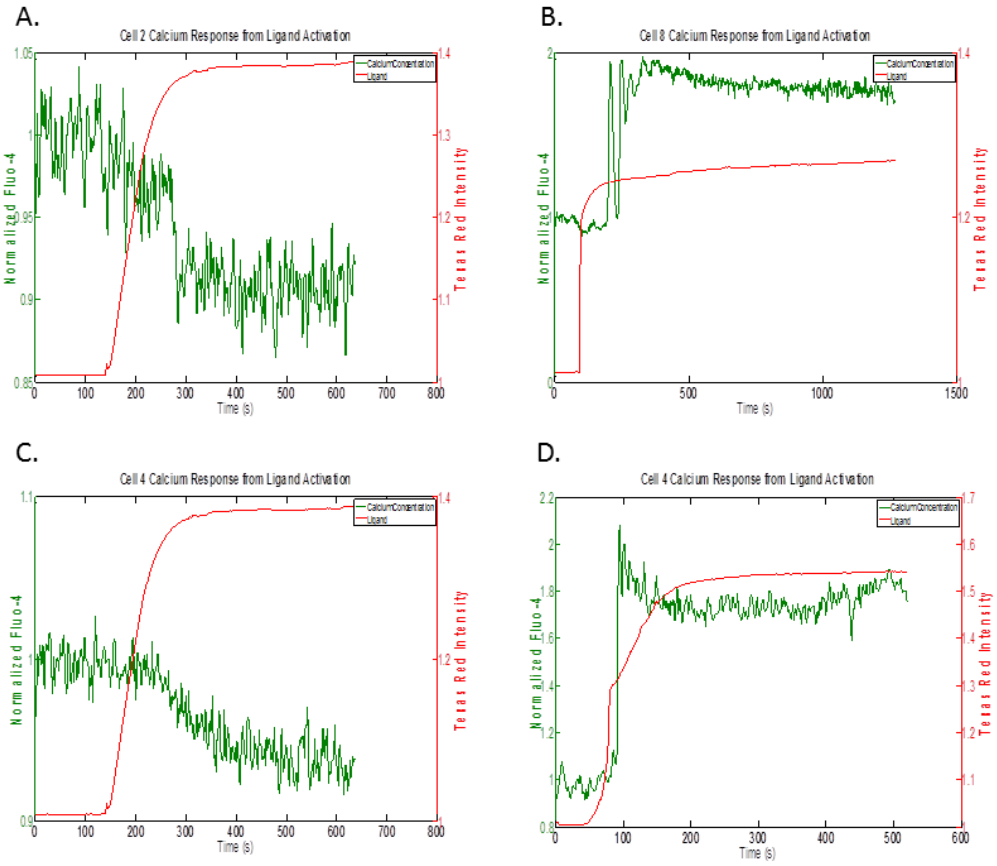

Figure 13. Positive and negative controls acquired. (A) and (C) Two types of controls were done, in the trap region. The first used no ligand in the stream that was pulsed to the trap region. The pulsed stream was brought to the cells for an infinite amount of time. The cells analyzed showed no activation due stream exposure, which is what should be expected. ((B) and D)) In the next control, DNP-BSA at a concentration of 1 µg/mL was pulsed to the trap region. The cells analyzed showed activation due to ligand exposure, which is what is expected.

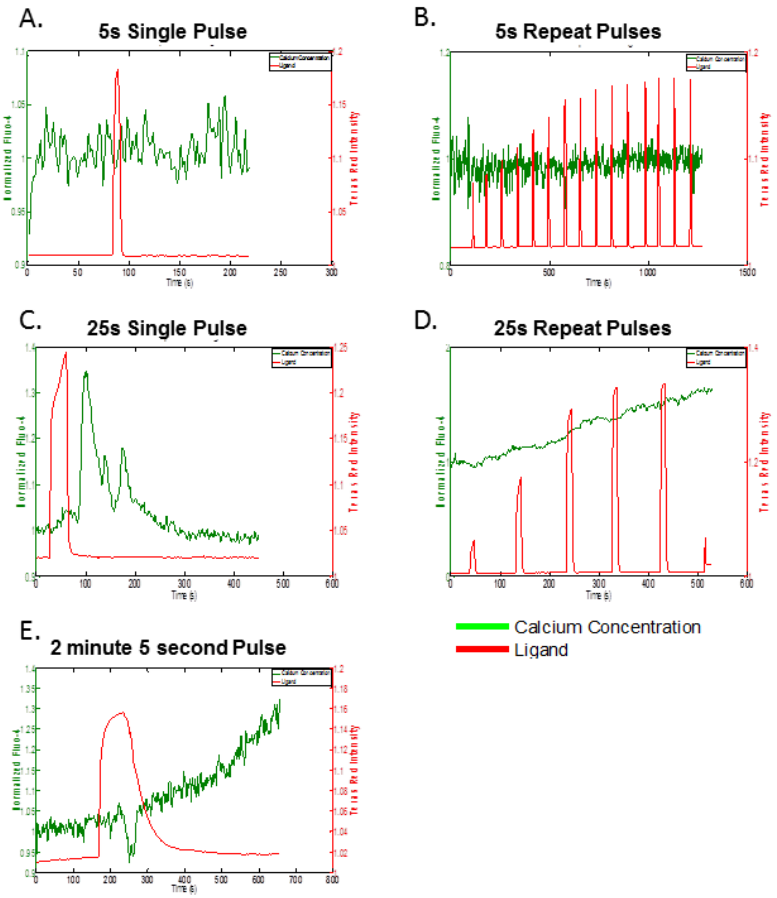

Figure 14. Five ligand pulse experiments. The five major ligand pulse experiments were conducted in the device. First the device was made ready for biologicals and loaded with cells. After loading cells, the ligand was brought into the device and by the trap area. Next, 1 µg/mL DNP-BSA ligand was pulsed toward the cells for a specific amount of time. A) The first type of pulse was for 5 seconds. This experiment showed no response through the data sets collected. B.) In a second experiment a 5 second pulse train experiment was conducted to the trapped cells. This experiment also showed no cellular response. C.) A third experiment was done where the ligand was pulsed for 25 seconds. This showed responses in some of the cells trapped. D.) A fourth type of experiment was conducted with a 25 second pulse train. This showed a different type of response which directly correlates to a steady increase in cytosolic calcium.. E.) Lastly, a 2 minute and 5 second pulse was conducted. The responses were similar to the responses seen in the 25 second pulse train experiments, just a less drastic response.

population of cells that responded. Finally a 2 minute and 5 second pulse experiment was conduction, which was designed by adding the five 25 second pulses together into one single pulse (Figure 14 E). This also showed a response from cells. The figures shown are indicative of the typical data collected for the particular experiment.

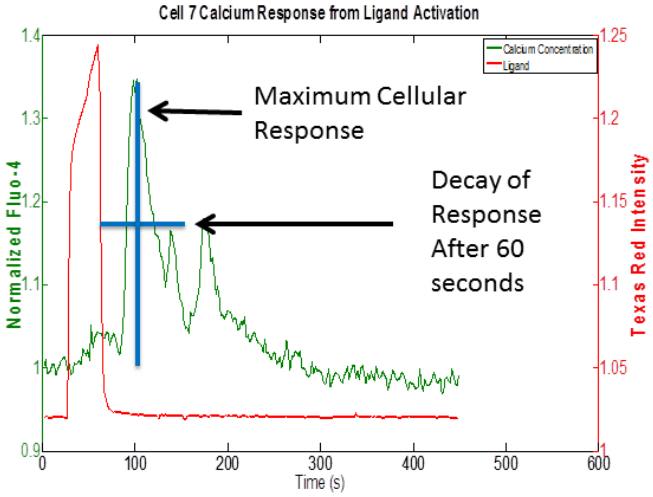

Figure 15. Data statistics collected. Statistics are taken from each cellular response. These statistics include first the maximum average response from a given experiment. Also included is the response decay after 60 seconds from a cell responding. Also included from the statistics were the number of experiments, number of days, number of cells, and the percent of cells that responded.

In order to characterize these data, we collected statistics from all data sets. More specifically, the data we collected included the maximum Fluo-4 intensity change which directly correlates to the maximum cytoplasmic calcium concentration change. The Fluo-4 decay in signal after 60 seconds from the initial increase of Fluo-4 signal was also collected from each cell (Figure 15). Statistics for total responders, number of experiments, number of cells imaged, and percentage responders was collected as well.

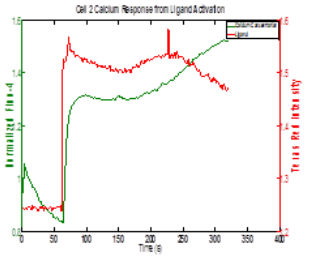

Figure 16. Data from cells grown on a coverslip and challenged with Ionophore. This data was taken on RBL cells grown on a coverslip and let adhere to the glass. Then they were incubated with Fluo-4 to track calcium (green). Next they were given ionophore (red) to exchange the calcium from stores to the cytosol A.) In experiments, cells showed an initial large increase in activation then a stable increase from there on.

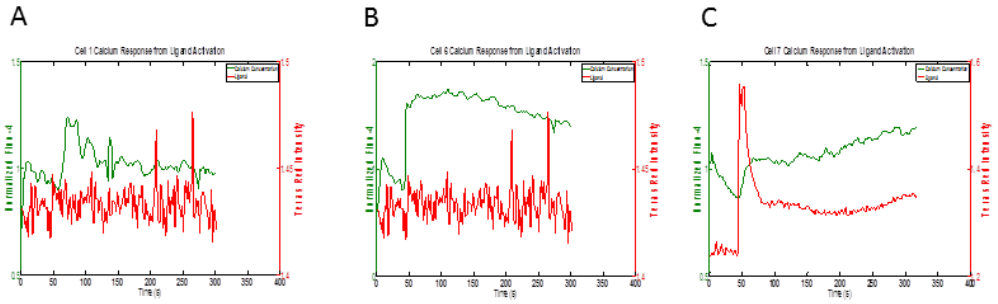

Figure 17. Data DNP-BSA crosslinking of cells grown on a coverslip. This data was taken with RBL cells grown on a coverslip so that the cells adhere to the glass. Then they were incubated with Fluo-4 (green) to track the calcium In the cytoplasm. Then 1 µg/mL DNP-BSA (red) was used to activate the cells. A.) In these experiments, there is a population of cells that has a spiked response due to ligand addition. B.) There was another population of cells that has a large increase in response after ligand addition with a steady response after the increase. C.) The third population had a gradual increase in response after ligand addition.

3.5. 8-Well Chamber Data Overview

To date, all calcium imaging has been performed on cells attached to a glass coverslide surface. So, the first control experiments that were conducted tested the calcium release of the FcεR1 receptor system in RBL cells attached to coverslips. I have used both calcium ionophore (A23187) and ligand (DNP-BSA) challenge to induce a calcium flux. In these experiments, the cells have responded as expected (compared to published results). The calcium movement is be monitored via Fluo-4 from the calcium stores. The addition of ionophore or ligand is monitored by detection of the Texas Red-conjugated BSA molecules in the solution.

Figure 16 shows the first round of control data taken in 8 well chambers. The cells in the

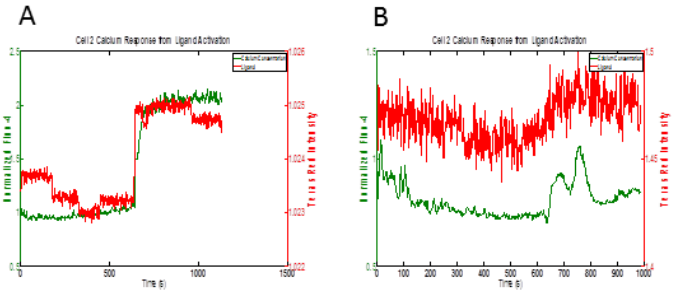

Figure18. Data taken from cells in the microfluidic device challenged with ionophore. This data was taken with RBL cell that have been loaded with Flou-4 (green). Then cells were brought into the device and let settle for a time in the device. They were given ionophore (red) and a response gathered. A.) Example of one cell that shows a large increase in response after ligand addition with a stable response after. The majority of cells responded in this manner B.) Another response gave a spiked response after ionophore addition.

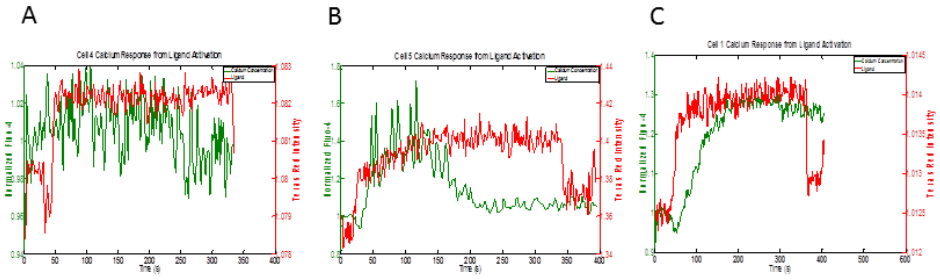

Figure19. Shear stress evaluation. RBL cells were loaded with Fluo-4 (green). They were brought into the device and left to take hold of the glass surface. Then flow was brought over them (red) and the shear stress data was collected by a change in fluorescence seen from buffer flowing across them. A.) One population of cells showed no response and most cells showed this type of response within this evaluation. B.) Another type response showed an increase in signal with a decay of signal after ligand exposure. C.) A third type of responses showed a rise in fluorescence after the shear flow begins then a stable signal after.

experiment were challenged with calcium ionophore and the movement of calcium was monitored as it is deposited in the cytoplasm from the cellular stores. These experiments yielded one type of trend in the data, cells increased in the cytoplasmic calcium concentration after ionophore addition. In a second control experiment, cells were challenged with DNP-BSA and the change in cytoplasmic calcium was measured. Three different responses was visualized, namely the cytoplasmic calcium showed a spiked response, a large increase in calcium levels or a slow increase over time due to ligand addition. (Figure 17 A, B, and C, respectively)

3.6 Microfluidic Device On Cover Glass Data Overview

The next controls completed were microfluidic device experiments. During the experiment, the cells were brought into the microfluidic device and given time to attach to the glass. Next either calcium ionophore, no DNP-BSA, or DNP-BSA was brought over the cells to test for calcium response due to shear flow, drug challenge, or FcεR1 receptor activation, respectively. Calcium ionophore addition showed two types of responses. One in which there was a large calcium response due to ligand exposure, shown in Figure 18A or a spike response after ligand exposure, shown in Figure 18B. Using no DNP-BSA showed the shear stress response to buffer flowing over cells. There are three types of responses in this case, one which shows no response due to ligand addition (Figure 19A), another which showed a slight response due to ligand exposure (Figure 19B), and a third that showed a larger response due to ligand

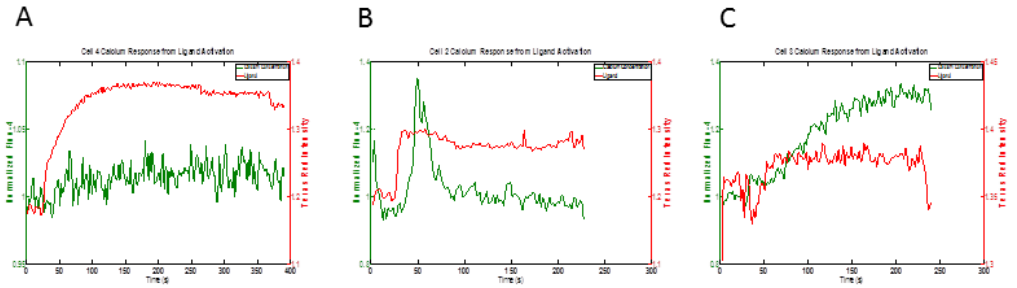

Figure 20. Data taken in the microfluidic device with DNP-BSA crosslinking. RBL cells were loaded with Flou-4 (green) and brought into the device. They are let settle on the glass surface, then 1 µg/mL DNP-BSA is directed to the cells (red), as a step function. A.) A population of cells showed no response from ligand exposure. B.) Another population shows a spiked response from ligand addition. C.) A third type of response shows a gradual raise in cellular activation due to ligand exposure.

exposure (Figure 19C). There was a larger amount of cells that didn't respond in this instance,

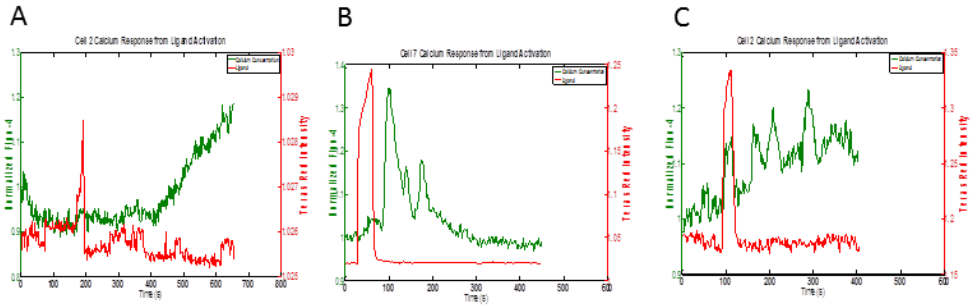

Figure 21. Single 25 second ligand pulse responses. RBL cells were loaded with Fluo-4 (green) then brought into the device. Then they were caught in the trap area and activated with 1 µg/mL DNP-BSA for 25 seconds. A.) One population of cells were lightly activated due to ligand exposure. This was the most common response collected from this experiment B.) A second population showed a spiked response from ligand exposure. C.) A third population showed a behavior change from stable calcium levels to oscillatory levels in the cytoplasm due to ligand exposure.

which is what we would expect. With DNP-BSA added to cells for an infinite amount of time there were three responses one in which there was no response (Figure 20 A), a spiked response

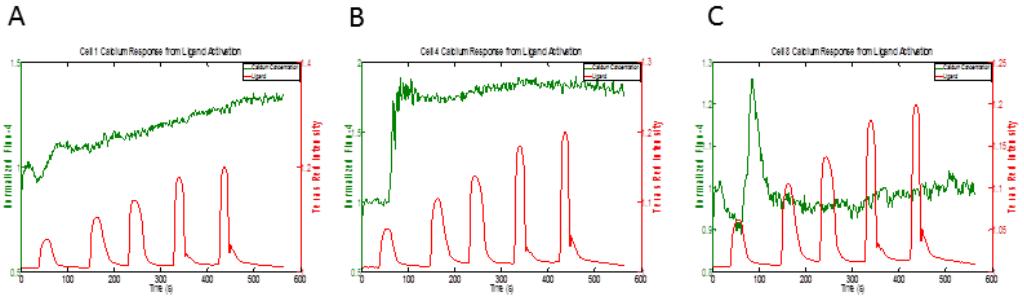

Figure22. 25 second repeat pulse experiments. RBLs cells were first loaded with Fluo-4 (green). The cells were then brought into the device and caught in the trap area. They were given five 25 second pulses at a concentration of 1 µg/mL DNP-BSA (red). The cellular responses were then collected. A.) One population of cells gave a light steady increase in cytoplasmic calcium due to the initial and continual ligand exposure. This was the response seen from most cells. B.) Another subset of cells showed a large increase in cellular response after the first ligand pulse and after a stable raised calcium level in the cytoplasm. C.) A third population showed a spiked response after the first ligand pulse.

A

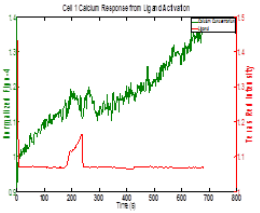

Figure 23. 2 minute and 5 second pulse experiments. RBL cells were loaded with Fluo-4 (green) and bought into the device. They were caught in the trap area and given a 2 minute and 5 second 1 µg/mL DNP-BSA pulse. This response was seen out of all the cells that responded. Namely it was a gradual raise in calcium response due to ligand exposure.

(Figure 20 B), and a response that showed a large increase after ligand exposure (Figure 20 C). In this case, the responses from cells outweigh the lack of response from cells which is what would be expected from this system.

3.7 Trap Region Microfluidic Device Data Overview

During the ligand pulse experiments in the microfluidic device, cells were captured in the trap region in the device. Then, the cells were exposed to 1 µg/mL DNP-BSA for 25 seconds using the pulse capability in the microfluidic device. Three types of responses where noted, one in which there was a small raise in calcium concentration due to ligand addition (Figure 21 A), another in which there was a spiked response due to ligand addition (Figure 21 B), and another which showed a change in calcium behavior after ligand addition (Figure 21 C). Majority of the cells showed a large increase in calcium after ligand addition which is very interesting.

Then 25 second pulse train experiments were conducted with a minute between the pulses widths. This experiment showed three types of responses again. One in which you have a steady increase after ligand pulses start (Figure 22 A). A second shows a large increase in calcium response after ligand addition on the first pulse (Figure 22 B). A third response showed a spike increase in calcium concentration after ligand addition. (Figure 22 C).

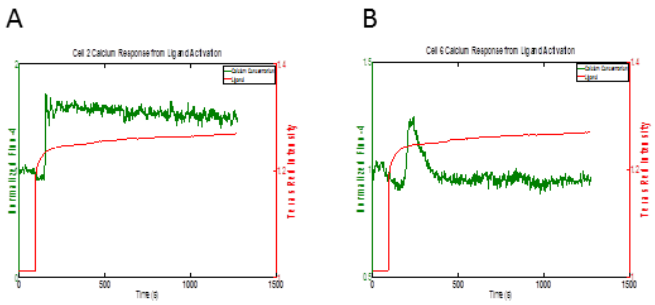

Figure 24. Step function pulse experiments. RBL cells are incubated with Fluo-4 (green) and brought into the device. Then they were caught in the trap area where they were given a step function pulse of 1 µg/mL DNP-BSA (red). A.) A population of cells showed an immediate raise in cytoplasmic calcium concentration after ligand exposure. This was the major response seen in this type of experiment. B.) A second response collected is a spiked response due to ligand exposure.

The next set of experiments were with a 2 minute and 5 second ligand pulse on RBL cells. This showed one particular response, which was a steady increase in calcium due to ligand addition (Figure 23 A). Throughout all of the experiments a positive control, where by cells were given ligand infinitely, was done to ensure the cells were behaving properly, this showed two types of responses. One of which was a large increase in calcium concentration due to ligand addition (Figure 24 A) and the second was a spiked response in calcium concentration due to ligand addition (Figure 24 B).

CHAPTER 4: DISCUSSION AND CONCLUSIONS

It is great to have a strong experimental baseline for new studies. In order to complete the specific aims we have identified, a microfluidic device was to be utilized. It was the key factor in conducting rapid delivery of stimulus to measure the calcium response of cells exposed to the by reagent delivery. To start off we conducted some coverslip experiments to test our process versus the literature. These experiments show all of the cells respond when given either ionophore or DNP-BSA. These responses are similar to those seen in Lee and Oliver's study at the 1 μg/mL DNP-BSA concentration. In the coverslip ionophore experiments we saw only a fast and high response. For the DNP-BSA stimulation, cells either responded fast and high, or with a spiked response. It is great to have data that is supported in past studies, because it shows we can recreate founded data and the experiments we conduct after are considered supported by that recreation.

The first aim, which was to characterize a microfluidic device for rapid delivery was initiated by some controls, conducted in the device. The next step was to ensure the behavior of the cells in the device did not deviate significantly from the cells activity out of the device. To do this the channel control experiments were conducted. A similar percentage of responders for the ionophore dosing was observed when compared to the coverslip control experiments. Specifically these cells showed either a high response, or a spike response. DNP-BSA stimulation showed a lower percentage of responders, however not as low as the microfluidic channel shear flow experiments. This is positive and what we should expect, as DNP-BSA addition should show more calcium movement from stores than purely shear flow stimulation. In the DNP-BSA incubation experiments a spiked response, a high response, or no response was seen. In the shear flow experiments a spiked response, a high response, or no response was caused. These controls show there is some difference in the behavior of the ligand to membrane protein interaction in the device when compared to the same proteins interacting in an 8-well chamber. This could be an effect of the difference in environment the cells are in, namely in the device the ligand is moving with directed motion by the cells, whereas the ligand in the 8-well chamber is moving in a diffusive manner by the cells. It may be that the smaller percentage of cells responding in the device is due to a population of cell never being affected by its

neighboring cells or not being activated by ligand due to these molecules moving with directed motion rather than diffusion. This could be an example of how degranulation from a cell can affect neighboring cells (Sudo, Tanaka et al. 1996, Liu, Barua et al. 2013).

To test the cell loading environment of the device the microfluidic trap control experiments were conducted. The first control tested how many cells were likely to be stimulated maximally by a step function pulse containing ligand. This showed a population of cells with a high response, a spiked response, or no response at all. The second control tested for shear flow activation, which was a step function pulse with no ligand. This experiment showed no responses. It is really supportive to know there were a higher percentage of responders with the step function containing ligand, and zero responders with step function pulse without ligand. These controls show that there is a similar percentage of cells responding by doing the same experiment with cells adherent to glass and in the devices channel, versus in suspension and caught in the trap area. Also it is very convincing to have the negative control contain no responders because that proves there is no shear flow activation when the cells are caught in the devices cell trapping area. You could arguably say the step function DNP-BSA pulse in the trap area activated more population of cells. This is exemplified by comparing the relative population of cells activated with DNP-BSA in the trap area and adhered to the channels glass surface. The baseline for activated cells due to shear flow is higher when the cells are attached to the glass surface, therefore the environment in the trap area is more conducive to activation of cells by ligand rather than by shear flow.

The next set of experiment tested the bandwidth of the system, and furthermore brought in the accomplishment of the second aim of this thesis. Namely Aim 2 was to measure the calcium response due to high time resolution of reagent delivery. To do that the first experiment done was the 25 second pulse which showed a variety of responses. There was a high response, a spiked response, an oscillatory response, or no response observed. Next the 25 second pulse train aimed to see if there was an additive effect to response with the five 25 second pulses. This experiment showed cells either had a gradual response, high response, spike response, or no response at all. This experiment did not show a significant difference in the amount of responders from the single 25 second pulse. The final experiment added up the five 25 second pulses in the 25 second pulse train for a 2 minute and 5 second pulse. This showed either a

gradual response or no response. These experiments holistically show the ligand incubation time directly effects the population of cells activated. This effect has been seen in the literature in Lee and Oliver's study. Although in their study the correlation shown is how ligand concentration is related to population of cells activated. The trend is the same in both cases, which indicates ligand incubation time or pulse time being positively correlated to ligand concentration. What is not conclusive in this study is the population of cells that are activated in the 25 second pulse, 25 second pulse train, and 2 minute 5 second pulse experiments. I would expect the correlation between these three experiments to hold true, but unfortunately is not true. This is because the large pulse had the least amount of cells respond and the 25 second pulse as well as the 25 second pulse train experiments had equal amounts of cells responding.

Table 1. Overview of Experiments and Responses. For each type of experiment parameters were pulled out and shown below. These parameters include the type of response tracked in a type of experiment, the number of experiments for the type of experiment. The number of days, number of cells were also collected for each experiment type. The average maximum value and decay after 60 seconds were also calculated for each experiment and where applicable (left to right).

Experiment	Set	experiments (#)	days (#)	cells (#)	average max (Normalized Intensity Counts)	Decay after 60s (Normalized Intensity Counts)	Percent responders (%)
Coverslip Ionophore	High and fast response	5	4	31	0.38		100
	No response	0	0	0	0.00		
	Overall	**5**	**4**	**31**			
Coverslip DNP-BSA	Spiked response	1	1	2	1.55	0.50	100
	High and fast response	1	1	4	2.00		
	Gradual Response	1	1	6	1.25		
	No response	0	0	0	0.00		
	Overall	**3**	**2**	**12**			
Microfluidic Channel	High response	2	1	11	1.75		100
	Spike response	1	1	2	1.30	0.50	

Ionophore	No response	0	0	0			
	Overall	**3**	**2**	**13**			
Microfluidic Channel DNP-BSA	Spike response	3	3	14	1.31	0.21	72
	High response	2	2	7	1.34		
	No response	3	3	8	0.00		
	Overall	**6**	**4**	**29**			
Microfluidic Channel Shearflow	Spike response	2	2	3	1.33	0.67	34
	High response	2	1	7	1.25		
	No response	5	4	19			
	Overall	**7**	**3**	**29**			
µfluidic Traps: Step Function Pulse	High and fast response	4	4	17	1.35		72
	Spike response	2	2	4	1.29	0.56	
	No response	4	4	8			
	Overall	**4**	**4**	**29**			
µfluidic Traps: No ligand, Step Pulse	No response	4	3	14			0
	Overall	**4**	**3**	**14**			
µfluidic Traps: 25 second pulse	High response	3	3	8	1.31		48
	Spike response	2	2	3	1.27	0.83	
	Oscillatory response	2	2	4	1.10		
	No response	5	4	16			
	Overall	**6**	**5**	**31**			
µfluidic Traps: 25 second train	Gradual Response	2	2	7	1.42		48
	High and fast response	1	1	1	1.90		
	Spike response	2	2	3	1.27	0.50	

	No response	3	2	12			
	Overall	**3**	**2**	**23**			
µfluidic Traps: 2 minute 5 second pulse	Gradual response	4	4	8	1.23		30
	No response	4	4	19			
	Overall	**4**	**4**	**27**			

In conclusion, this research is the start of testing the information bandwidth of the calcium signaling system as affected by FcεR1 receptor stimulation in the suspended RBL cells. These data show that the control tests for the calcium signaling system match the data in the literature for the specific concentration used when cells are out of the microfluidic device. Also what is exemplified in the data is the cells behavior in suspension versus adhered to glass and the behavior of cells in a grouped population versus singled out. Overall it is shown that there is a lowered number of cells that respond due to a similar amount of ligand stimulation inside versus outside of the device, respectively. The cells in the device were also singled out from the population, which is a difference the device can offer from experiments on coverslip. The cells that were experimented on in the device seemed to respond less when given the same ligand stimulation. This could be an example of how degranulation from a cell can activate a response from neighboring cells (Sudo, Tanaka et al. 1996, Erlich, Yagil et al. 2014). In any case, these data suggest all responses seen with cells caught in the trap region are valid. This is due to both the positive and negative controls showing an amount of cells responding which is above and below, respectively, the amount of cells responding in any of the trap experiments.

CHAPTER 5: FUTURE WORK

This study leaves some possible questions that when answered, will further elucidate the cell signaling system being investigated. Conducting an experiment to find the amount of available receptors of the cells that are caught in the trap region would be advantageous for future applications of this device. This could alude to a better handle over how many receptors one cell has available compared to another cells. This could be tested by loading cells into the traps then bringing in fluorescent IgE and seeing where that IgE binds to the cell. Then the receptor density can be calculated by fluorescence. Another experiment that could add to clarity of the experiment in this thesis would be using a lower concentration of DNP-BSA to find the level which shows a 25 second response that is different from the 25 second pulse train response. Finding a concentration of DNP-BSA that will show this will unlock more answers regarding the systems bandwidth than the IgE concentration used currently in experiments. A third thing would be to collect more control data to get a larger population of cells to analyze.

Possible other directions this research could take includes conducting this research with strict control over the IgE incubation time on the cells. The concentration and time of ligand incubation could be varied in these experiments. Another experiment that could be done is to let the cells experience a ligand, DF3 or DNP-BSA, at an initial time then wait a day or a week and give the same cells another dosage at the same concentration and same incubation time to see the variability in response when comparing those two time points. Essentially this would be an initial step to characterizing the diminishing effects of ligand addition on cells. This would be a more relevant biological problem than current methods in this field. Moreover, this would be really interesting as much of the environment in the microfluidic device is controlled; like the temperature, gas, and nutrients in the immediate environment of the cells. This microfluidic environment almost mimics the environment of the body. The reason being the body holds an approximate temperature of 37^{o}C and so does the microfluidic device. The microfluidic device is pressurized with any mixture of gas, with a mixture of CO_2 you can mimic what is present during cell culture conditions. A constant flow of media, which contains salts, glucose, growth factors and other contents to keep cells as healthy as if they were in a mammal. Cells in suspension or

non-suspension can also be investigated, so human mast cells can be used for experiments in this microfluidic device.

CHAPTER 6: REFERENCES

Amatore, C., S. Arbault, Y. Chen, C. Crozatier and I. Tapsoba (2007). "Electrochemical detection in a microfluidic device of oxidative stress generated by macrophage cells." Lab Chip 7(2): 233-238.

Andrews, N. L., K. A. Lidke, J. R. Pfeiffer, A. R. Burns, B. S. Wilson, J. M. Oliver and D. S. Lidke (2008). "Actin restricts FcepsilonRI diffusion and facilitates antigen-induced receptor immobilization." Nat Cell Biol 10(8): 955-963.

Anup K Singh, T. M., Jean-Loup Faulon, Chris Apblett, Mark van Benthem, Cathy Branda, Steve Branda, Allan Brasier, Jim Brennan, Susan Brozik, Elizabeth Carles, Amanda Carroll-Portillo, Bryan Carson, Ryan Davis, Elsa Ndiaye-Dulac, Jean-Loup Faulon, Paul Gemperline, David Haaland, Amy Herr, Conrad James, Howland Jones, Jaewook Joo, Julie Kaiser, Glenn Kubiak, Todd Lane, Diane Lidke, Ron Manginell, Shawn Martin, Milind Misra, Matt Moorman, Jaclyn Murton, Kamlesh Patel, Thomas Perroud, Steve Plimpton, Jens Poschet, Roberto Rebeil, Susan Rempe, Ron Renzi, Bryce Ricken, Ken Sale, William Seaman, Mike Sinclair, Nimisha Srivastava, Dan Throckmorton, Meiye Wu, Zhaoduo Zhang (2009). Microscale Immune Studies Laboratory.

Barker, S. A., D. Lujan and B. S. Wilson (1999). "Multiple roles for PI 3-kinase in the regulation of PLC gamma activity and Ca2+ mobilization in antigen-stimulated mast cells." Journal of Leukocyte Biology 65(3): 321-329.

Cefaliello, C., M. Eyman, D. Melck, R. De Stefano, E. Ferrara, M. Crispino and A. Giuditta (2014). "Brain Synaptosomes Harbor More Than One Cytoplasmic System of Protein Synthesis." Journal of Neuroscience Research 92(11): 1573-1580.

Chalmers, M., M. J. Schell and P. Thorn (2006). "Agonist-evoked inositol trisphosphate receptor (IP3R) clustering is not dependent on changes in the structure of the endoplasmic reticulum." Biochem J 394(Pt 1): 57-66.

Cohen, R., A. Torres, H. T. Ma, D. Holowka and B. Baird (2009). "Ca2+ waves initiate antigen-stimulated Ca2+ responses in mast cells." J Immunol 183(10): 6478-6488.

Di Carlo, D. and L. P. Lee (2006). "Dynamic single-cell analysis for quantitative biology." Analytical Chemistry 78(23): 7918-7925.

Erlich, T. H., Z. Yagil, G. Kay, A. Peretz, H. Migalovich-Sheikhet, S. Tshori, H. Nechushtan, F. Levi-Schaffer, A. Saada and E. Razin (2014). "Mitochondrial STAT3 plays a major role in IgE-antigen-mediated mast cell exocytosis." The Journal of allergy and clinical immunology 134(2): 460-469.e410.

Fowlkes, V., C. G. Wilson, W. Carver and E. C. Goldsmith (2013). "Mechanical loading promotes mast cell degranulation via RGD-integrin dependent pathways." J Biomech 46(4): 788-795.

Gee, K. R., K. A. Brown, W. N. Chen, J. Bishop-Stewart, D. Gray and I. Johnson (2000). "Chemical and physiological characterization of fluo-4 Ca(2+)-indicator dyes." Cell Calcium 27(2): 97-106.

Gimborn, K., E. Lessmann, S. Kuppig, G. Krystal and M. Huber (2005). "SHIP down-regulates Fc epsilon R1-induced degranulation at supraoptimal IgE or antigen levels." Journal of Immunology 174(1): 507-516.

Gomez-Sjoeberg, R., A. A. Leyrat, D. M. Pirone, C. S. Chen and S. R. Quake (2007). "Versatile, fully automated, microfluidic cell culture system." Analytical Chemistry 79(22): 8557-8563.

Gustavsson, A. K., D. D. van Niekerk, C. B. Adiels, M. Goksor and J. L. Snoep (2014). "Heterogeneity of glycolytic oscillatory behaviour in individual yeast cells." FEBS Lett 588(1): 3-7.

Han, A. and A. B. Frazier (2006). "Ion channel characterization using single cell impedance spectroscopy." Lab Chip 6(11): 1412-1414.

Hartmann, A., M. Stamp, R. Kmeth, S. Buchegger, B. Stritzker, B. Saldamli, R. Burgkart, M. F. Schneider and A. Wixforth (2014). "A novel tool for dynamic cell adhesion studies--the De-Adhesion Number Investigator DANI." Lab Chip 14(3): 542-546.

Hersen, P., M. N. McClean, L. Mahadevan and S. Ramanathan (2008). "Signal processing by the HOG MAP kinase pathway." Proc Natl Acad Sci U S A 105(20): 7165-7170.

Huh, D., H. J. Kim, J. P. Fraser, D. E. Shea, M. Khan, A. Bahinski, G. A. Hamilton and D. E. Ingber (2013). "Microfabrication of human organs-on-chips." Nat Protoc 8(11): 2135-2157.

James, C. D., M. W. Moorman, B. D. Carson, C. S. Branda, J. W. Lantz, R. P. Manginell, A. Martino and A. K. Singh (2009). "Nuclear translocation kinetics of NF-kappaB in macrophages challenged with pathogens in a microfluidic platform." Biomed Microdevices 11(3): 693-700.

James, C. D., N. Reuel, E. S. Lee, R. V. Davalos, S. S. Mani, A. Carroll-Portillo, R. Rebeil, A. Martino and C. A. Apblett (2008). "Impedimetric and optical interrogation of single cells in a microfluidic device for real-time viability and chemical response assessment." Biosens Bioelectron 23(6): 845-851.

Jayasinghe, I. D., M. Munro, D. Baddeley, B. S. Launikonis and C. Soeller (2014). "Observation of the molecular organization of calcium release sites in fast- and slow-twitch skeletal muscle with nanoscale imaging." Journal of the Royal Society Interface 11(99): 40570-40570.

Lee, R. J. and J. M. Oliver (1995). "ROLES FOR CA2+ STORES RELEASE AND 2 CA2+ INFLUX PATHWAYS IN THE FC-EPSILON-R1-ACTIVATED CA2+ RESPONSES OF RBL-2H3 MAST-CELLS." Molecular Biology of the Cell 6(7): 825-839.

Liu, Y. L., D. Barua, P. Liu, B. S. Wilson, J. M. Oliver, W. S. Hlavacek and A. K. Singh (2013). "Single-Cell Measurements of IgE-Mediated Fc epsilon RI Signaling Using an Integrated Microfluidic Platform." Plos One 8(3): 12.

Mahajan, A., D. Barua, P. Cutler, D. S. Lidke, F. A. Espinoza, C. Pehlke, R. Grattan, Y. Kawakami, C. S. Tung, A. R. M. Bradbury, W. S. Hlavacek and B. S. Wilson (2014). "Optimal Aggregation of Fc epsilon RI with a Structurally Defined Trivalent Ligand Overrides Negative Regulation Driven by Phosphatases." Acs Chemical Biology 9(7): 1508-1519.

Memon, A. A., M. Munk, E. Nexo and B. S. Sorensen (2011). "Calcium-induced apoptosis is delayed by HER1 receptor signalling through the Akt and PLC gamma pathways in bladder cancer cells." Scandinavian Journal of Clinical & Laboratory Investigation 71(1): 45-51.

Mettetal, J. T., D. Muzzey, C. Gomez-Uribe and A. van Oudenaarden (2008). "The frequency dependence of osmo-adaptation in Saccharomyces cerevisiae." Science 319(5862): 482-484.

Mirasoli, M., M. Guardigli, E. Michelini and A. Roda (2014). "Recent advancements in chemical luminescence-based lab-on-chip and microfluidic platforms for bioanalysis." J Pharm Biomed Anal 87: 36-52.

Muzzey, D. and A. van Oudenaarden (2009). "Quantitative time-lapse fluorescence microscopy in single cells." Annu Rev Cell Dev Biol 25: 301-327.

Sanchez-Gonzalez, P. (2010). "Calmodulin-mediated regulation of the epidermal growth factor receptor (vol 277, pg 327, 2010)." Febs Journal 277(6): 1583-1583.

Sawano, A., S. Takayama, M. Matsuda and A. Miyawaki (2002). "Lateral propagation of EGF signaling after local stimulation is dependent on receptor density." Developmental Cell 3(2): 245-257.

Shackman, J. G., G. M. Dahlgren, J. L. Peters and R. T. Kennedy (2005). "Perfusion and chemical monitoring of living cells on a microfluidic chip." Lab Chip 5(1): 56-63.

Silverman, M. A., J. Shoag, J. Wu and G. A. Koretzky (2006). "Disruption of SLP-76 interaction with Gads inhibits dynamic clustering of SLP-76 and FcepsilonRI signaling in mast cells." Mol Cell Biol 26(5): 1826-1838.

Sudo, N., K. Tanaka, Y. Koga, Y. Okumura, C. Kubo and K. Nomoto (1996). "Extracellular ATP activates mast cells via a mechanism that is different from the activation induced by the cross-linking of Fc receptors." Journal of Immunology 156(10): 3970-3979.

Suzuki, Y., T. Yoshimaru, T. Inoue and C. Ra (2006). "Mitochondrial Ca2+ flux is a critical determinant of the Ca2+ dependence of mast cell degranulation." J Leukoc Biol 79(3): 508-518.

Szallasi, Z., J\, \#246, r. Stelling and V. Periwal (2006). System Modeling in Cellular Biology: From Concepts to Nuts and Bolts, The MIT Press.

Tarn, M. D., M. J. Lopez-Martinez and N. Pamme (2014). "On-chip processing of particles and cells via multilaminar flow streams." Anal Bioanal Chem 406(1): 139-161.

Tourovskaia, A., X. Figueroa-Masot and A. Folch (2005). "Differentiation-on-a-chip: a microfluidic platform for long-term cell culture studies." Lab Chip 5(1): 14-19.

Tshori, S. and E. Razin (2010). "Editorial: Mast cell degranulation and calcium entry--the Fyn-calcium store connection." J Leukoc Biol 88(5): 837-838.

Warkiani, M. E., G. Guan, K. B. Luan, W. C. Lee, A. A. Bhagat, P. K. Chaudhuri, D. S. Tan, W. T. Lim, S. C. Lee, P. C. Chen, C. T. Lim and J. Han (2014). "Slanted spiral microfluidics for the ultra-fast, label-free isolation of circulating tumor cells." Lab Chip 14(1): 128-137.

Weltin, A., K. Slotwinski, J. Kieninger, I. Moser, G. Jobst, M. Wego, R. Ehret and G. A. Urban (2014). "Cell culture monitoring for drug screening and cancer research: a transparent, microfluidic, multi-sensor microsystem." Lab Chip 14(1): 138-146.

Wheeler, A. R., W. R. Throndset, R. J. Whelan, A. M. Leach, R. N. Zare, Y. H. Liao, K. Farrell, I. D. Manger and A. Daridon (2003). "Microfluidic device for single-cell analysis." Analytical Chemistry 75(14): 3581-3586.

Whitesides, G. M., E. Ostuni, S. Takayama, X. Y. Jiang and D. E. Ingber (2001). "Soft lithography in biology and biochemistry." Annual Review of Biomedical Engineering 3: 335-373.

Yang, W. Z., J. Y. Chen and L. W. Zhou (2009). "Effects of Shear Stress on Intracellular Calcium Change and Histamine Release in Rat Basophilic Leukemia (RBL-2H3) Cells." Journal of Environmental Pathology Toxicology and Oncology 28(3): 223-230.

Zhao, X., F. Xu, L. Tang, W. Du, X. Feng and B. F. Liu (2013). "Microfluidic chip-based C. elegans microinjection system for investigating cell-cell communication in vivo." Biosens Bioelectron 50: 28-34.